International Journal of Rock Mechanics & Mining Sciences 194 (2025) 106208

Contents lists available at ScienceDirect

International Journal of Rock Mechanics and Mining Sciences

journal homepage: www.elsevier.com/locate/ijrmms

Controls of lithological heterogeneity on self-sealing behavior of propped fractures in Marcellus shale

Zeynal Abiddin Erguler [a,b,*], Derek Elsworth [a]

[a] Department of Energy and Mineral Engineering, G3 Center, Penn State University, University Park, PA, 16802, USA
[b] Geological Engineering Department, Kütahya Dumlupınar University, 43100, Kütahya, Türkiye

ARTICLE INFO

Keywords:
Marcellus shale
Self-sealing
Shale gas
Shale hydration
Slaking

ABSTRACT

Developments in drilling technology and hydraulic fracturing methods have made shale formations an important geo-energy source and repository for energy-related wastes. Their very low permeability and outstanding potential for self-sealing are assets in sequestering wastes, but a limitation in sustaining shale gas production. We measure the permeability and self-sealing evolution of proppant-filled fractures in Marcellus shale, including the effect of time, normal stress, loading and unloading conditions, temperature and fluid composition. Permeabilities are measured over a first cycle of 24 h, with a hiatus of 56–91 days, and then remeasured to define impacts of physicochemical degradation (slaking) in a second cycle. Permeability reduces by up to 63 % where proppant crushing is isolated as a mechanism in embedment-eliminated steel split cores. In shales, lithological heterogeneity causes micro-slaking of clay-rich laminae appearing as stripes on the proppant oriented parallel to bedding planes with different proppant embedments resulting in differentiation in initial permeability values at the same proppant loading concentration. Intact rock compaction and mechanical closure-based self-sealing reduces permeability between 7.7 % and 21.6 % with an average value of only 14.5 %. Slaking, embedment, and swelling behavior in the Marcellus shale are responsible for all of the other remaining reductions in permeability. The reductions in permeability during all loading conditions correlate exponentially with time and can be defined by a single relation. The dimensionless constants of this equation depend on normal stress, physicomechanical properties and effective aperture. Long-term permeability measurements in a second cycle after 56–91 days show self-sealing through mineral precipitation in the Marcellus shale with a cohesive layer in the otherwise cohesionless proppant. The significant reductions between the initial and the second cycle permeability measurements reveal that time is a significant controlling factor in the self-sealing behavior of Marcellus shale in terms of reflecting creep deformation, slaking, and long-lasting geochemical processes.

1. Introduction

Intensive scientific and engineering studies have focused on unconventional energy sources such as shale oil, natural gas, shale gas and tight sand gas. In particular, significant progress has been made in recent years in the implementation of hydraulic fracturing and horizontal drilling. In addition, in recent years, geological units, particularly clay-bearing rock units (e.g., Opalinus clay and Boom clay, e.g. Nussbaum et al.[1]) have been seen as potential host for storing nuclear waste due to their low permeability and self-sealing characteristics of discontinuities. Self-sealing and fracture closure are crucial for the safe storage of nuclear waste as these processes cause a dramatic decrease in the conductivity of propped fractures.[2–4] This loss in conductivity[5]) results from a drop in the reservoir pressure and increase in effective stress and as a result of creep closure with time.[6] Similar to the outputs of experimental investigations performed by Barree et al.[7] and Palisch et al.,[3] Yu et al.[4] measured a 95 % reduction in conductivity when the effective stress was increased to 48 MPa, with this effect continuing but waning with further stress increase.

The closure of cracks formed in shale formations by natural processes is directly dependent on the percentage and type of clay minerals[8] contained in the rock units. High stress causes a significant permeability decrease in clay-rich shales due to the altering of rock strength and susceptibility to proppant embedment.[4,9,10] If the percentage of clay minerals is below a threshold, the self-sealing of cracks does not occur. This threshold value is approximately 40 %[11] from studies conducted in

* Corresponding author. Geological Engineering Department, Kütahya Dumlupınar University, 43100, Kütahya, Türkiye.
E-mail address: zeynal.erguler@dpu.edu.tr (Z.A. Erguler).

https://doi.org/10.1016/j.ijrmms.2025.106208
Received 15 May 2025; Received in revised form 29 June 2025; Accepted 1 July 2025

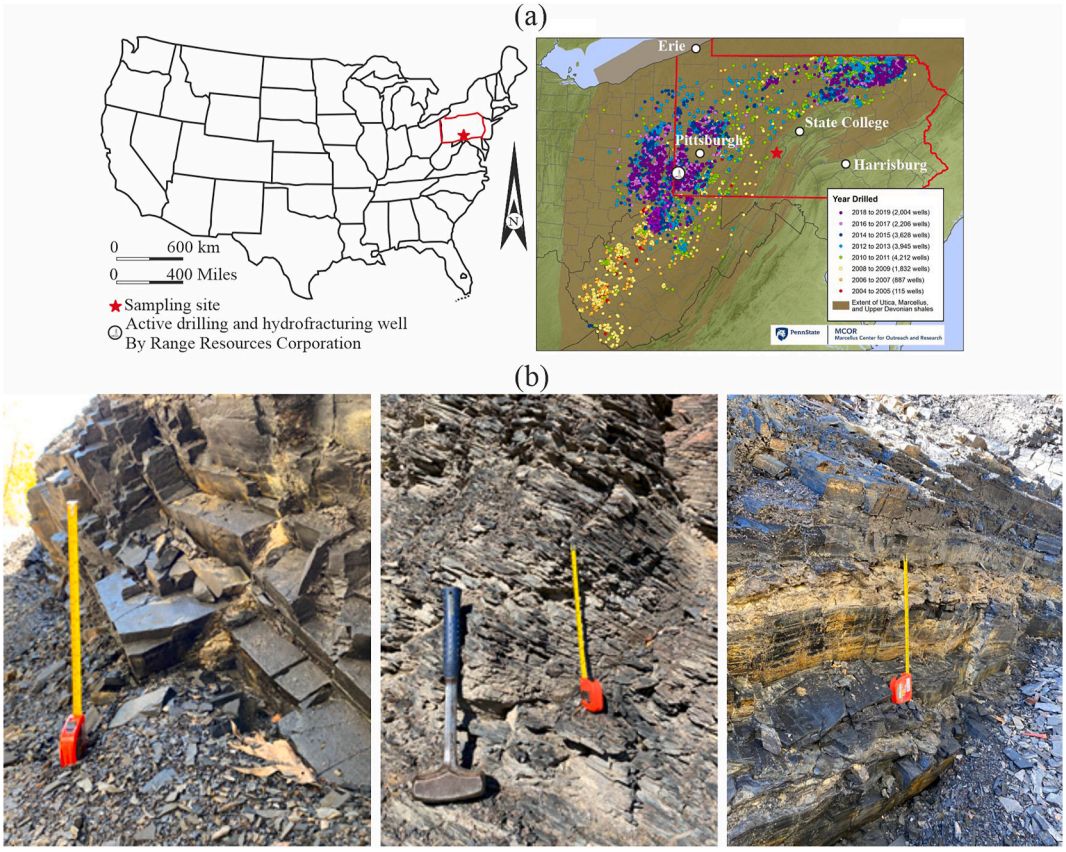

Fig. 1. a) Sampling site (coordinates: 40.435286° by −78.342129°) and unconventional wells drilled in Pennsylvania, Ohio, and West Virginia from 2004 to December 31, 2019 (data from the Pennsylvania Department of Environmental Protection, West Virginia Department of Environmental Protection and Ohio Division of Oil and Gas Resources collected and mapped by The Marcellus Center for Outreach and Research (MCOR) at Penn State University), b) Typical images taken from the outcrop of fresh and heavily disintegrated Marcellus gas shale formation.

the hydrocarbon industry[12] - clay contents for Marcellus (>50 %)[13,14] exceed these critical values. Several factors control the self-sealing behavior of clayey rocks. These are the mechanical properties of both rocks and proppant (e.g., proppant embedment, crushing, compaction and rearrangement and pack concentration).[4,8,15–21] Several closure mechanisms exist,[11] including: (1) compaction of rock matrix due to compression, (2) mechanical crack closure due to an increase in normal stress, (3) crack closure due to shear and the creation of wear products, (4) closure due to creep, (5) swelling, (6) slaking and (7) the formation of new minerals. Previous studies (El Sgher et al.[22] Boosari et al.[23]) considered the increase in the effective stress with fluid pressure drawdown and the resulting decrease in fracture apertures in numerical modelling of unconventional reservoirs. Besides the significant contributions originating from deformations due to normal and shear stresses and by creep, the swelling of Opalinus and Boom clays is the most important self-sealing mechanism.[24] However, the closure of hydraulically induced cracks in shale gas formations is quite different from that in the clay-rich rocks considered for storing nuclear waste - in terms of rheology and stress conditions.[24] In addition, compared with the Opalinus and Boom clays as clay-bearing rocks considered for nuclear waste repositories, shale formations show a lithologically anisotropic geological composition over very short length scales. Shale gas formations are typically heterogeneous from nanometer to meter scale,[13] and changes in bedding thickness and mineralogical composition can sometimes be critical in terms of swelling and other self-sealing mechanisms.

Furthermore, the heterogeneity of the shale formations also affects fracture propagation.[22] The presence of brittle minerals (large-grained quartz, feldspar, and calcite) and clay minerals bearing layers is a significant factor affecting its microstructure (Gu et al.[25]), leading to the difference in mechanical properties. Lithological heterogeneity and anisotropic mechanical characteristics of shale are discussed extensively in previous studies.[26–32] However, few references[33,34] address the importance of lithological heterogeneity on the self-sealing response of shales. This heterogeneity limits the use of outputs obtained from relatively strong cores of previous studies[4,35] since these bias sampling by under-sampling soft and friable strata that are not readily recovered. Thus, preserved carbonate-rich and durable parts of the stratigraphic section do not generally include the heterogeneous composition and highly anisotropic compositions that readily disintegrate.

Self-sealing in clay-rich rocks is a complex natural process that depends on many mechanisms and is controlled by many factors. We overcome the sampling bias that limits testing on clay-rich samples by combining Marcellus shale samples with very high clay content Opalinus clay from Mont Terri (Switzerland). Permeability tests were performed on composite samples with Opalinus upstream and Marcellus downstream to investigate the self-sealing behavior of the Marcellus shale by considering all controlling factors such as time, normal stress, loading condition, temperature, and aqueous fluid composition. The effects of these controlling parameters on the self-sealing properties of this shale gas formation are comprehensively evaluated in this study.

2. Materials and methods

2.1. Field investigation and sampling

Considering its importance for shale gas production, and particularly the published data related to unconventional drilled wells given in Fig. 1a, the self-sealing properties of the Marcellus shale formation are

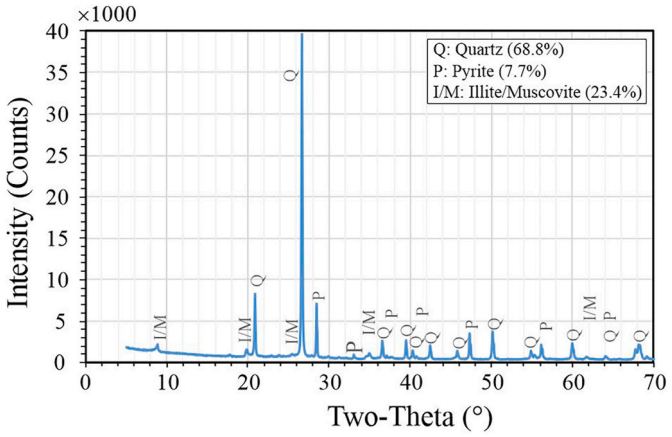

Fig. 2. Typical X-ray diffraction pattern and mineralogical composition of the Marcellus shale.

Table 1
Rlemental composition of Marcellus shale based on the SEM–EDS microanalyses.

Element	Apparent concentration	Wt (%)	Atomic (%)	Standard name
C	2.46	18.93	28.35	C Vit
O	38.90	42.59	47.88	SiO_2
Mg	0.35	0.33	0.25	MgO
Al	5.26	4.72	3.15	Al_2O_3
Si	31.30	28.66	18.36	SiO_2
S	1.09	1.19	0.67	FeS_2
K	1.57	1.50	0.69	KBr
Ti	0.20	0.23	0.09	Ti
Fe	1.12	1.27	0.41	Fe
Cu	0.48	0.57	0.16	Cu

investigated in this study. We recover block samples of Marcellus shale from outcrop at Frankstown, Pennsylvania (New Enterprise quarry off Locke Mountain Road in Frankstown). The form of this Marcellus shale outcrop is shown in Fig. 1b. Considering the lithologically heterogeneous structure of the Marcellus shale formation, block samples were taken from rock units having a potentially wide range of self-sealing behaviors. Two joint sets, with mean discontinuity spacings of 18 cm and 17 cm, are present, in addition to the bedding plane (N48W/29NE). Weathering on the discontinuity surfaces was observed as yellow, brown and dark brown, dark grey and black. The Marcellus shale cleaves along the relatively flat and smooth bedding planes where very thin clay laminae are present. Heavily disintegrating sequences resulting from stress release and weathering were detected in strata with high clay content in the near-surface. However, slaking potential decreases rapidly with depth due to the decreasing effect of wetting-drying and freeze-thaw cycles. While clayey infilling materials were detected in the open fractures, calcite precipitation, expected to form over geological time, could not be detected macroscopically. Three different Marcellus shale blocks were recovered to evaluate the propensity for self-sealing. In addition to field investigation and sampling at the Marcellus shale outcrop, the ongoing operation of an active deep drilling and hydro-fractured well in Claysville, PA (USA) (Fig. 1a) provided a downhole in situ temperature of ~60 °C.

2.2. Mineralogical and geomechanical properties of samples

The fine-grained clastic extrabasinal particles and organic-rich pelagic intrabasinal remains forming the lithological characteristics of the Marcellus shale were deposited in an anoxic marine basin during the Middle Devonian as a result of the activity of the Acadian Orogeny.[36] Various investigations define its physical, structural, mineralogical and mechanical properties. Based on XRD and XRF techniques, Hupp and Donovan[36] identified nine mineral phases (quartz, muscovite, illite, pyrite, chlorite, albite, calcite, dolomite, barite). The total organic carbon content of this shale changes between 2 % and 20 %,[22] while the

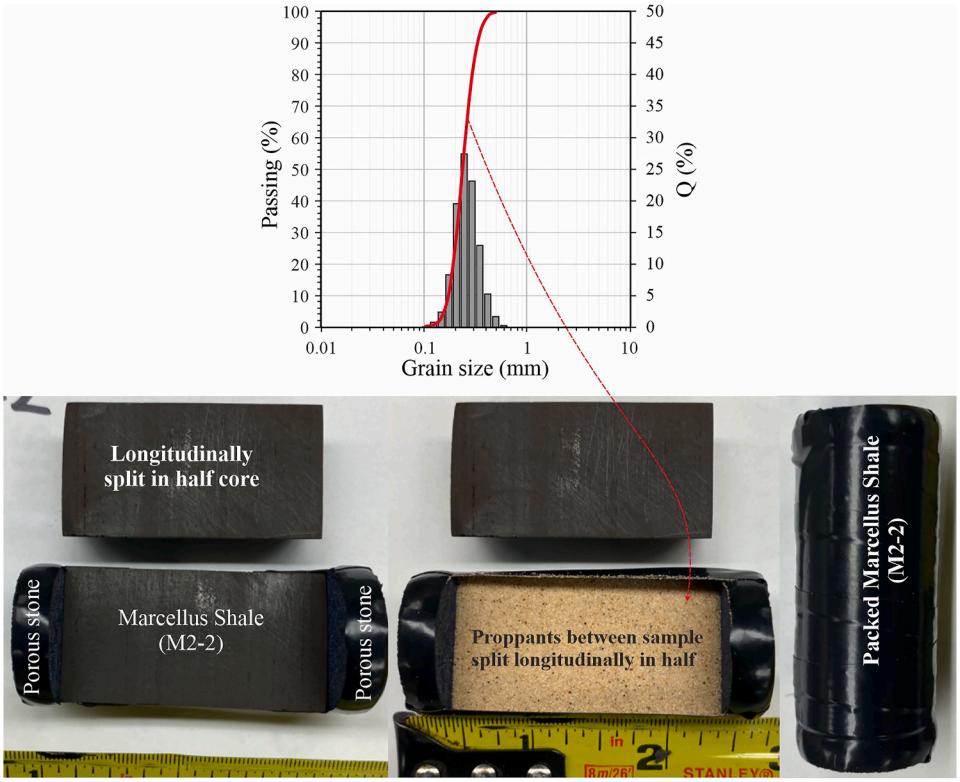

Fig. 3. Grain size distribution curve for proppant and its placement between two halves of a core sample split longitudinally before the permeability test.

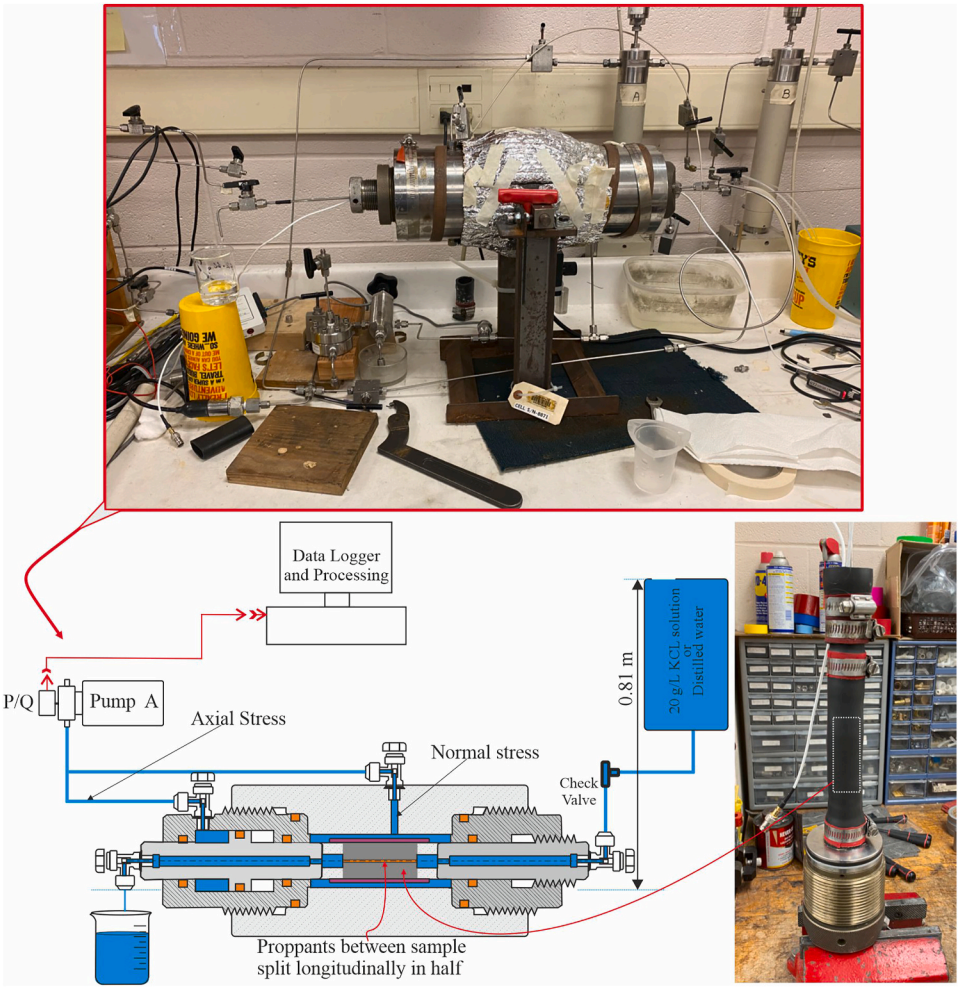

Fig. 4. Experimental setup to measure permeability characteristics of split shale samples.

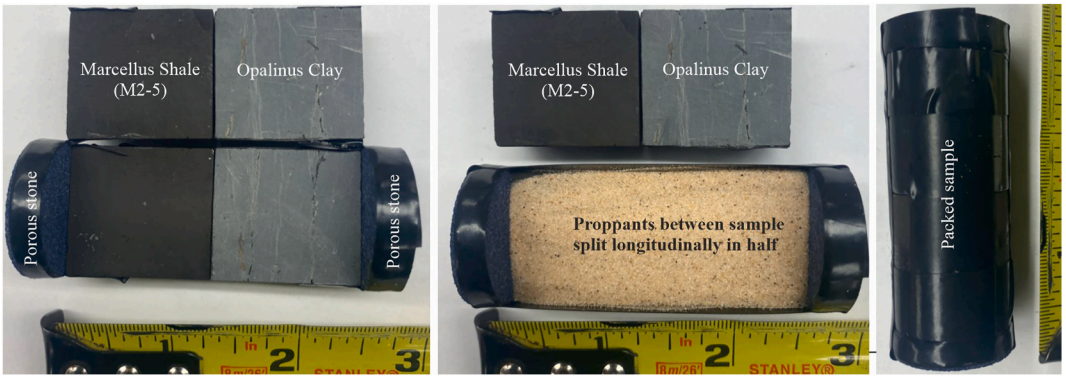

Fig. 5. The use of Opalinus clay to simulate and upscale the impact of slaking and particle ejection into the flowfield on the self-sealing behavior of fractures in Marcellus.

total content of carbonate minerals ranges from 0 to 59 %.[37] Brunauer and Smosna[38] found that the clay mineral content of Marcellus shale changes between 10 % and 35 %, with the percentage of non-swelling minerals (quartz and feldspar) ranging from 10 % to 60 %. However, the clay content of the Marcellus formation can reach 52 %[14] for some strata rich in clay minerals. Such percentages are important in understanding the effects of all factors, particularly swelling and slaking, on the self-sealing of fractures. Quartz, muscovite, kaolinite and pyrite are the main mineralogical constituents of Marcellus shale; the percentages of these minerals based on XRD analyses were determined (Yu et al.[35] as 43.4 %, 46.8 %, 5.1 %, and 4.7 %, respectively. Yu et al.[4] used Marcellus samples that contain (XRD) 60.2 % quartz, 20.5 % muscovite, 13.5 % nacrite, 4.3 % pyrite and 1.5 % clinochlore. Static Poisson ratio and Young's modulus of Marcellus shale are 0.16–0.18[39] and 15.5 GPa,[40] respectively. In addition to previously obtained mineralogical compositions for the Marcellus shale, we powdered our samples and collected diffraction data from 5 to 70° 2θ using a Malvern Panalytical Empyrean® instrument fitted with a copper (Kα1-2 = 1.540598/1.544426 Å)

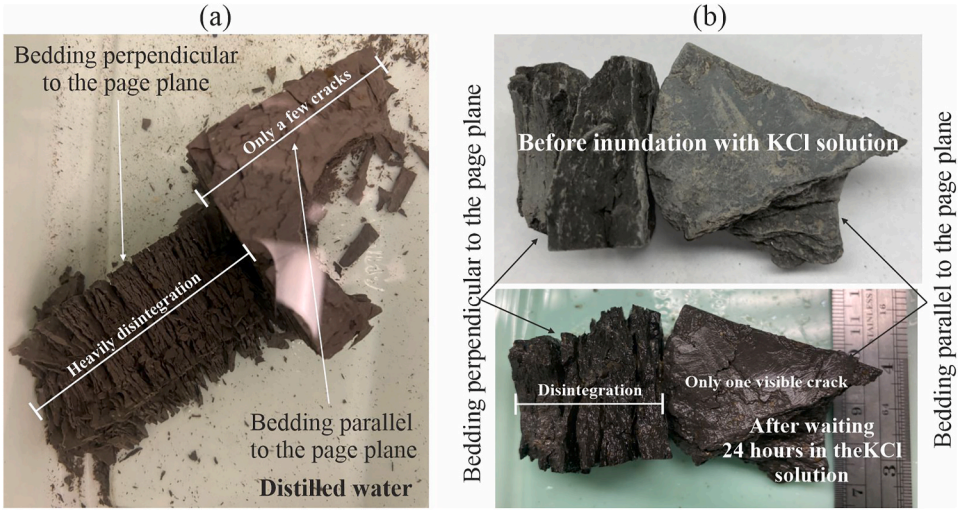

Fig. 6. Slaking-dependent cracking parallel to the bedding plane for Opalinus clay after waiting 24 h for saturation by a) Distilled water, and b) KCl solution.

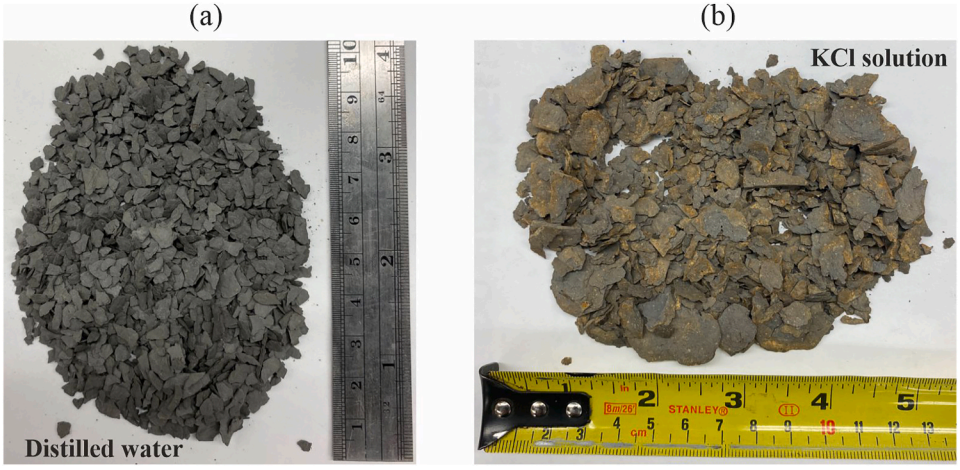

Fig. 7. Disintegration of Opalinus clay after applying the fourth cycle of a) Distilled water, and b) KCl solution.

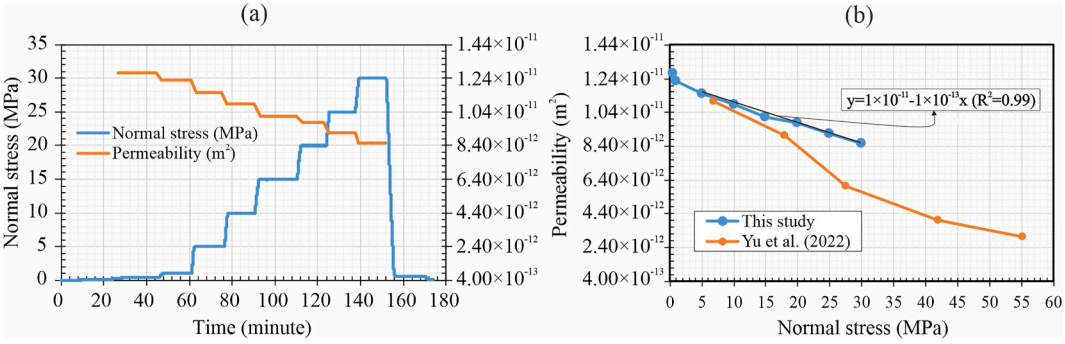

Fig. 8. a) Time-dependent variation in normal stress and permeability, b) Relationships between normal stress and permeability for propped steel-walled fracture with a proppant concentration of 2.44 kg/m^2.

long-fine-focus X-ray tube operated at 45 kV and 40 mA. As shown in Fig. 2, our Marcellus shale is mainly composed of Quartz, illite/-muscovite, and pyrite with percentages of 68.8, 23.4, and 7.7, respectively. Calcite, dolomite, and chlorite were not detected from XRD analyses. Besides this analysis, SEM–EDS microanalyses were also performed across the fresh surface of Marcellus shale, with the results given in Table 1.

The physicochemical properties of Jurassic-aged Opalinus clay (Mont Terri, Switzerland) were investigated by Thury and Bossart,[41] Bossart et al.,[42] and Bossart and Thury[43] in detail. Opalinus clay, specified as claystone, is typically composed of 65 % clay minerals and 35 % non-clay minerals (20 % quartz, 7 % calcite, 3 % feldspar, 2 % siderite, 1 % dolomite, 1 % pyrite).[44]

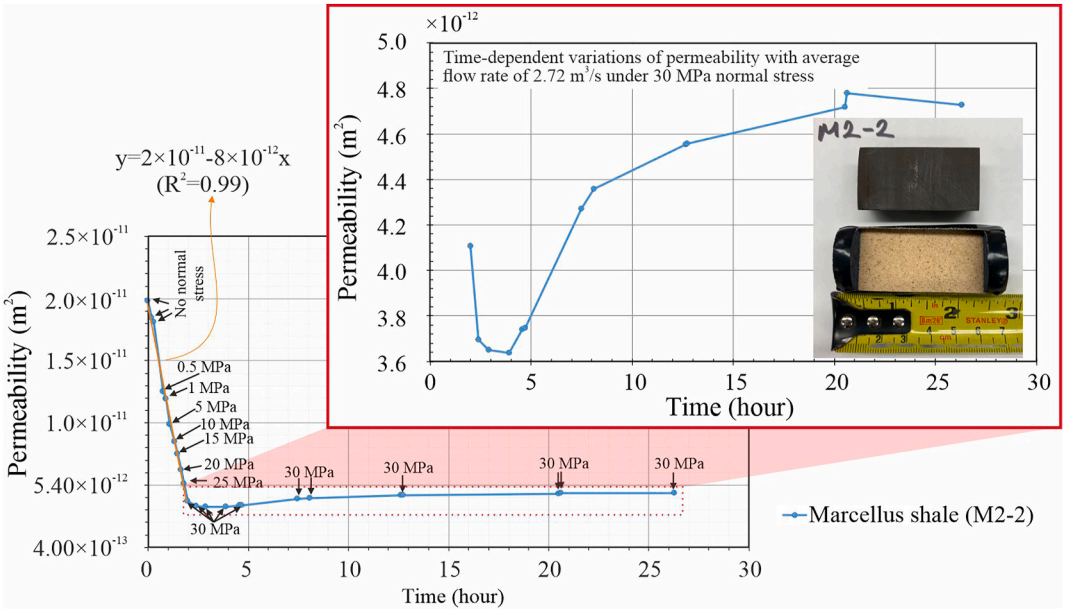

Fig. 9. Impact of internal erosion of disintegrated particles and proppants on initial permeability measurement under very low flow rate and upstream pressure.

2.3. Induced fracture characteristics, proppants and core sample preparation for testing

The pore size of micro-fractures and organic pores within shale reservoir vary between 1–3 nm and 400–750 nm, with an average of 100 nm.[45] During hydraulic fracturing, cracks having a typical aperture ranging from a few sand grains to a maximum of 12 mm are formed,[46] and extend between 100 and 200 m.[47] Various studies[20,48–54] investigate the effect of proppants on proppant-pack permeability by considering particularly particle size, strength and concentration of proppants. The proppant embedment-based decreases in the conductivity percentages are measured at 65.9 % and 87.5 % for proppant concentrations of 10 kg/m^2 and 5 kg/m^2, respectively.[51] Proppant embedment causes conductivity loss in the case of induced fractures within rocks having a static modulus of elasticity lower than 13 GPa.[48] The effect of roughness on the conductivity of the propped fracture decreases at higher proppant concentrations.[20] To examine the effect of proppant loading concentration on the conductivity of propped fractures under different effective stresses, Yu et al.[4] performed a series of laboratory tests using proppant loading concentrations of 0.49, 1.22, 2.44, and 4.88 kg/m^2. They note that increasing proppant loading concentration decreases the embedment depth through a more uniform stress distribution applied to the fracture face – absent stress concentrations. This outcome was verified by experimental results, empirical correlations (Kozeny-Carman equation) and numerical approaches[53] emphasizing that shale hydration significantly influences proppant embedment. An increase in proppant concentration increases fracture conductivity.[4,53] Moreover, the conductivity of Marcellus shale remains approximately constant over different stress ranges when using high proppant loading concentration due to reduced proppant embedment.[4] In addition, a multilayer distribution provides more contact points to distribute stress and reduces crushing. Based on these previous studies, we use a quartz sand proppant concentration of 2.44 kg/m^2 to prevent proppant embedment and proppant breakage and to obtain a fracture aperture to represent fractures at a mass of 0.33g per layer.[4] Thus, using a mass of 3.05 g of proppant in this study provides ~9–10 proppant layers. The grain size distribution curve of this proppant is given in Fig. 3. The core samples, which had lengths and diameters of 50 mm and 25 mm, respectively, were extracted from two Marcellus blocks showing relatively different disintegration behavior in the field condition. As seen in Fig. 3, the core samples were longitudinally split and sandwiched the proppant pack. Significant sample loss occurred both during coring and splitting due to the ready disintegration of these weak clayey rocks. Therefore, hand tools and equipment such as handsaws and sandpaper were used to prepare cores from some weak clay-containing rocks. Before permeability tests, the fractured surfaces of the split samples were ground using #180 grit sandpaper to obtain surfaces with similar roughnesses. To obtain parallel surfaces and so ensure uniform loading conditions, the upper and lower surfaces of the cores were similarly abraded with the same sandpaper. The placement of proppants in the longitudinally split shale cores is given in Fig. 3.

2.4. Slaking tests

"Body" and "surface" slaking[55–57] are the main mechanisms effectively controlling the self-sealing of fractures. When clayey rocks come into contact with water, repulsive forces form between the clay particles due to the swelling of the double-layer structure. If these repulsive forces are sufficient to break diagenetic bonds then very thin clay bands break off on the fracture surfaces and disperse within the voids in the proppant pack.[11] This mechanism can cause significant occlusion of the proppant pack over time and, therefore, economically significant decreases in shale gas production. A fluid with a specific chemical composition can also be used to prevent shale slaking and so limit clogging by induced fractures with disintegrated tiny shale particles during and after fracturing. Potassium chloride (KCl) brine with a concentration of 20 g/L, is representative of flowback fluids obtained from the different unconventional shale plays.[4] However, in addition to hard layers, shale formations are also composed of weak strata containing very high concentrations of clay minerals. Thus, relative controls of water and brine on slaking characteristics was investigated using both distilled water and 20 g/L KCl solution.

Jar slake tests,[58] slake index tests[59] and slake durability tests[60] are generally utilized in defining the slaking characteristics of rocks. Although the slake durability test is widely used, it has important limitations, such as mechanical disintegration from comminution. Therefore, particularly to remove the effect of mechanical breakdown-related mass loss, the jar slake test (wetting and drying cycles) was used to determine the slaking behavior of selected samples. For this purpose, rock fragments with masses ranging from 34 to 247 g were subjected to wetting and drying cycles with mass loss measured at the end of each wetting and drying cycle.

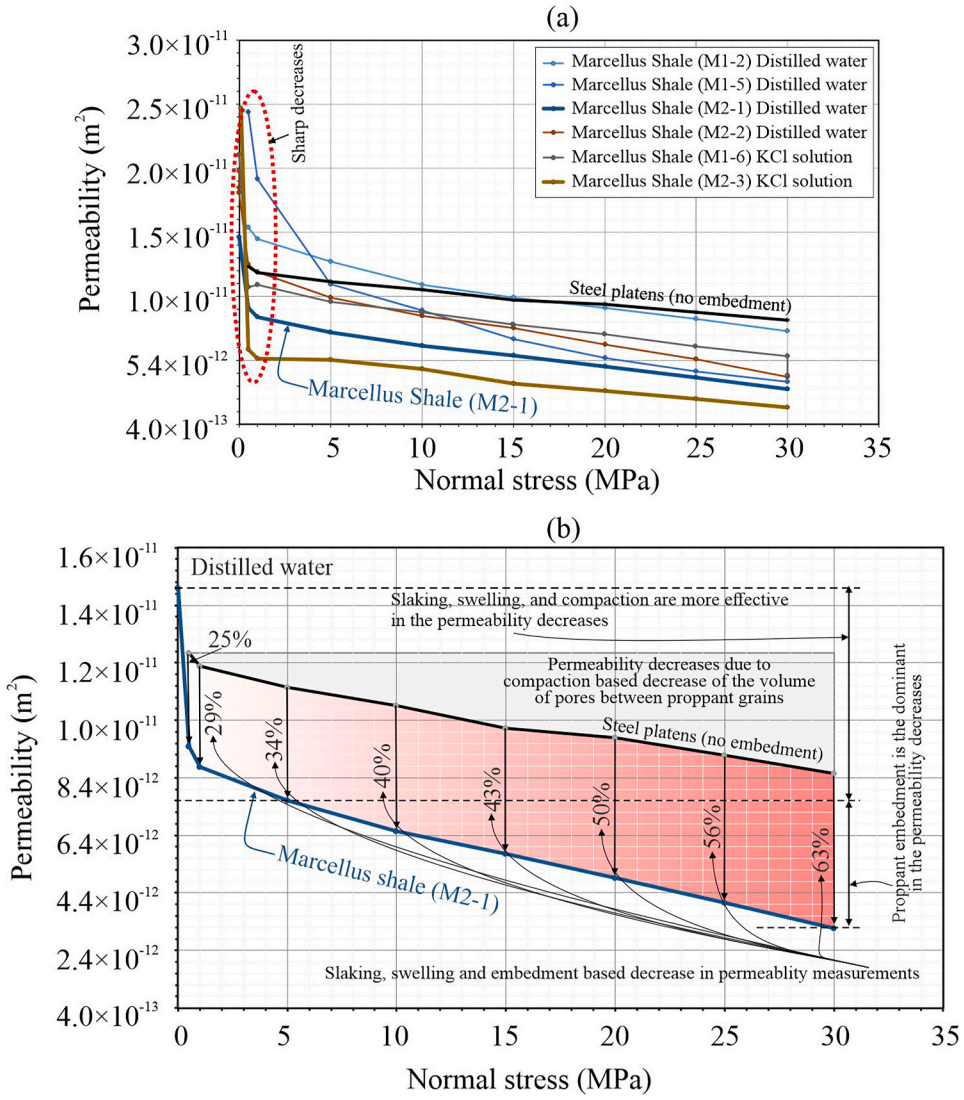

Fig. 10. a) Relationships between normal stress and permeability during triaxial loading, b) Typical example of decrease in permeability due to slaking, swelling, and proppant embedment processes.

2.5. Measurement of time-dependent permeabilities of induced fractures

We use a triaxial coreholder permeameter (Fig. 4) to measure the self-sealing characteristics of the shales. We use a split steel core with lengths and diameters of 50 and 25 mm to measure embedment-free permeability. Difficulties associated with keeping the upstream and downstream pressures constant in the high-pressure-capacity pumps made the control of pressure gradients challenging. Problems in the erosion of proppant particles at low stresses were overcome by using a low pressure gradient with ~7.95 kPa upstream pressure discharging to atmospheric pressure downstream. All permeability tests were carried at room temperature with normal stresses between 0.5 MPa and 30 MPa. To see the effect of time and temperatures on the self-sealing properties of rocks, these split samples subjected to the first permeability cycle were kept in water with temperatures of 50 °C–80 °C and then tested again at room temperature. In addition to these modifications to the second cycle of permeability measurements, fractured Opalinus clay was added upstream to understand the effect of heterogeneous geological structure on self-sealing behavior in the Marcellus Shale. The sample preparation stages used for this purpose are given in Fig. 5.

Both distilled water and 20 g/L KCl solution were used as permeants to understand the self-sealing characteristics of shales, with permeability (k) calculated based on Darcy's law, as,

$$k\ (m^2) = \frac{\mu \times L}{w} \times \frac{Q}{\Delta P} \times \frac{\rho_{bulk}}{c_p} \quad (1)$$

where is μ is the viscosity of water (9.544×10^{-4} Pa × s), L is the length of the flow path, w is the flow path width, Q is the flow rate (m^3/s), and ΔP (Pa) is the pressure differential between the upstream and downstream of the packed split core. ρ_{bulk} is proppant bulk density (1630 kg/m^3) and c_p is proppant loading concentration (2.44 kg/m^2) to define approximate fracture aperture.

3. Results and discussion

We observe significant impacts of slaking behavior for both Marcellus and Opalinus shales exposed to distilled water and KCl brine. We examine these impacts on permeability evolution in propped fractures by isolating the effects of proppant embedment and slaking through successive experiments. We factor out the impacts of proppant embedment through experiments with steel split cores. First cycle experiments are conducted with propped fractures in Marcellus, followed by long-term exposure to water before recommencing flowthrough experiments with upstream fractures in Opalinus clay as a slaking agent.

Table 2
Data fit empirical relations linking permeability and normal stress obtained from the first cycle of experiments.

Split samples	Normal stress	Fluid	Empirical equations
Steel platens	Loading	Distilled water	$k = 1.2 \times 10^{-11}$ -1.2 × $10^{-13}\sigma$ ($R^2 = 0.99$)
Marcellus Shale (M1-2)	Loading	Distilled water	$k = 1.4 \times 10^{-11}$ -2.1 × $10^{-13}\sigma$ ($R^2 = 0.98$)
Marcellus Shale (M1-5)	Loading	Distilled water	$k = 1.2 \times 10^{-11}$ -3.1 × $10^{-13}\sigma$ ($R^2 = 0.96$)
Marcellus Shale (M2-1)	Loading	Distilled water	$k = 0.8 \times 10^{-11}$ -1.7 × $10^{-13}\sigma$ ($R^2 = 1.00$)
Marcellus Shale (M2-2)	Loading	Distilled water	$k = 1.2 \times 10^{-11}$ -2.4 × $10^{-13}\sigma$ ($R^2 = 1.00$)
Marcellus Shale (M1-4)-Opalinus Clay	Loading	Distilled water	$k = 2.1 \times 10^{-12}$ -1.2 × $10^{-13}\sigma$ ($R^2 = 0.90$)
Marcellus Shale (M2-5)-Opalinus Clay	Loading	KCl solution	$k = 9.7 \times 10^{-12}$ -2.0 × $10^{-13}\sigma$ ($R^2 = 0.98$)
Marcellus Shale (M1-6)	Loading	KCl solution	$k = 1.1 \times 10^{-11}$ -1.7 × $10^{-13}\sigma$ ($R^2 = 1.00$)
Marcellus Shale (M2-3)	Loading	KCl solution	$k = 0.6 \times 10^{-11}$ -1.5 × $10^{-13}\sigma$ ($R^2 = 0.99$)
Marcellus Shale (M2-2)	Unloading	Distilled water	$k = 5.4 \times 10^{-12}$ -2.5 × $10^{-14}\sigma$ ($R^2 = 0.93$)
Marcellus Shale (M1-6)	Unloading	KCl solution	$k = 3.7 \times 10^{-12}$ -5.4 × $10^{-14}\sigma$ ($R^2 = 0.93$)
Marcellus Shale (M2-3)	Unloading	KCl solution	$k = 1.9 \times 10^{-12}$ -1.7 × $10^{-14}\sigma$ ($R^2 = 0.95$)
Marcellus Shale (M2-5)-Opalinus Clay	Unloading	KCl solution	$k = 3.2 \times 10^{-12}$ -3.6 × $10^{-14}\sigma$ ($R^2 = 0.91$)

k: permeability (m^2), σ: normal stress (MPa).

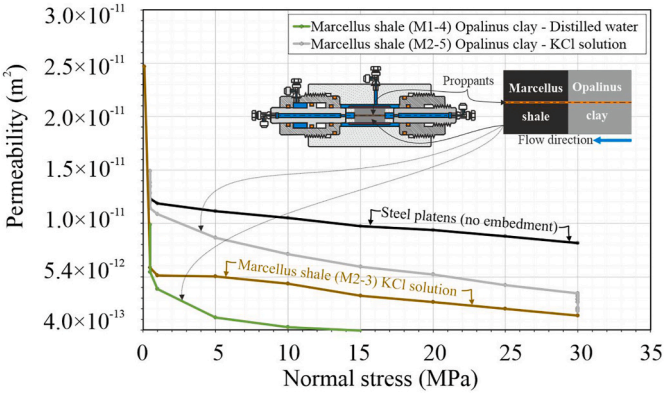

Fig 11. Effect of heterogeneous geological structure on self-sealing behavior of Marcellus shale.

3.1. Effects of distilled water and KCl solution on slaking behavior

Initial slaking experiments define that the mass loss of relatively durable Marcellus shale inundated with distilled water ranges between 0.3 % and 1.8 %. The durable samples, when subjected to the KCl solution, show reduced slaking behavior but with salt precipitated within the resulting cracks. Disintegration of the Opalinus clay advances considerably more rapidly and completely with diagenetic bonds broken during the first wetting-drying cycle for rocks with high clay contents. As seen in Fig. 6, numerous cracks form with a preferential alignment in the direction of the bedding, but are limited in the direction perpendicular to the bedding. This rapidity of slaking is an indicator of how rapidly permeability may be impacted for the propped fractures. The disintegration characteristics of these weak samples in the KCl solution were quite different from those in distilled water (Fig. 7).

3.2. Permeability measurement absent embedment (steel platens)

We explore the impact of embedment on the evolution of permeability in propped fractures by first eliminating its effect. This is completed by measuring the permeability of a proppant pack sandwiched within a split steel core. The permeability of a propped fracture in steel split core for normal stresses in the range of 0.5–30 MPa and a proppant concentration of 2.44 kg/m^2 changes between 1.19 × 10^{-11} m^2 and 7.97 × 10^{-12} m^2 with an average value of 9.92 × 10^{-12} m^2 (Fig. 8). Fig. 8a shows the time-dependent variation in normal stress and permeability and the relationships between normal stress and permeability with the same proppant concentration of 2.44 kg/m^2 obtained by Yu et al.[4] are given in Fig. 8b.

Permeability decreases linearly with increasing normal stress (Fig. 8b), without proppant crushing resulting in the absence of any rapid drop. While approximately similar results were obtained by Yu et al.[4] at low normal stress, the difference between the two permeability measurements significantly increases with increasing normal stress.

3.3. Initial permeability measurements

3.3.1. Effect of micro-slaking on self-sealing evolution

Similar to other clay-rich rocks, the Marcellus shale disintegrates due to natural weathering (Fig. 1 b) with the same slaking behavior observed in laboratory tests. Shale hydration is a major cause of proppant embedment[53] and is readily determined from slake durability tests (e.g., Franklin and Chandra[60]). However, it is difficult to measure the impact of micro-slaking that occurs as a result of contact with water – and this may occur even at low flow velocities. We measure permeability with continuous water flow at a rate of 2.72 m^3/s under low constant upstream pressure of 7.95 kPa. The time-dependent variation in permeability of this packed shale core (Fig. 9) shows a linear decrease for the first 2 h (119 min) as normal stress is linearly increased with time, with a very high coefficient of determination (R^2) (from 0 to 30 MPa normal stress). The effective stress-based decrease in permeability continues for another 2 h at a constant normal stress of 30 MPa. However, approximately 4 h later, the permeability eventually starts to increase.

We attribute this small increase in permeability to the erosion of fine-grained material from the system. To prevent such internal erosion of disintegrated particles and to so create self-sealing conditions, the water flow was retained only for approximately 10 min of the permeability test duration while performing the remaining tests. As seen in Fig. 9, the permeability stabilizes only after ~24 h.

3.3.2. Effect of normal stress on self-sealing evolution

To determine the effect of distilled water and KCl brine on self-sealing using multiple Marcellus core samples. Marcellus shale cores were subjected to permeability tests under a low constant upstream pressure provided by both distilled water and KCl brine. The relationships between normal stress and initial permeability obtained during the loading stage are given in Fig. 10a. Although a proppant concentration of 2.44 kg/m^2 was selected in all experiments, the beginning permeability values at low normal stress show broad scatter. In addition to differences in the beginning permeabilities, significant sharp decreases in permeability were observed in the first 2–5 MPa of normal stress, where slaking, swelling, and stress-induced self-sealing processes are expected to be more effective.

The scatter in the initial permeabilities (Fig. 10a) clearly reveals the sensitivity of the results to fabrication of the initial sample. As shown in Fig. 10a, the normal stress-dependent changes in permeability (up to 5 MPa) and the relationship beyond this stress are also highly variable among experiments. Very rapid decreases were measured in permeability values to 5 MPa normal stress. Above this stress threshold, there are strong and statistically significant linear relationships between normal stress and permeability (Table 2). The Marcellus shale shows very low mass loss after the fourth cycle of slaking tests. However, when

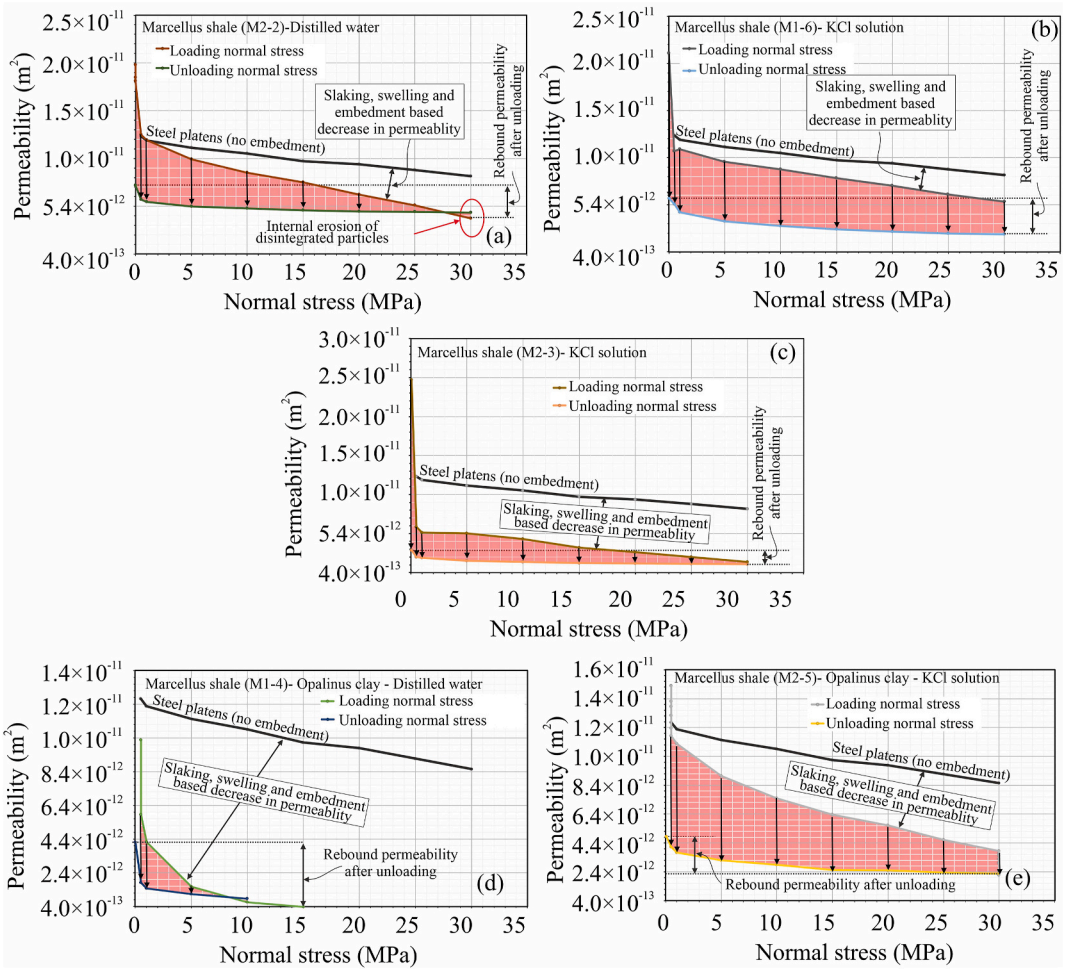

Fig. 12. Relationships between normal stress and permeability during loading and unloading.

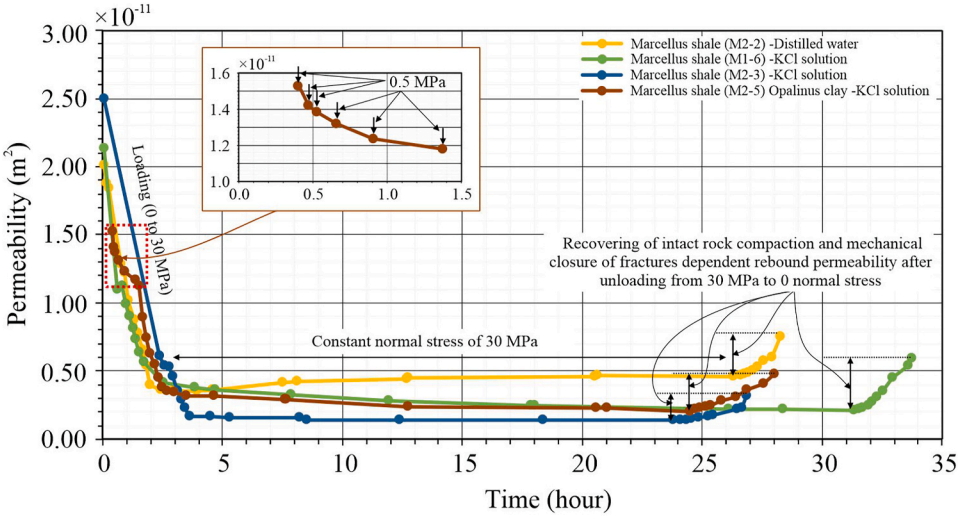

Fig. 13. Initial permeability changes of the propped fracture during loading and unloading.

the normal stress-dependent permeability measurements of steel platens (no embedment) are considered (Fig. 10b), it is apparent that even relatively durable shales exhibit significant self-sealing behavior due to slaking, swelling, and proppant embedment. Taking the results obtained from steel platens as reference, the decrease in permeability reaches ~63 % in some samples (Fig. 10b). Slaking, swelling, and compaction are more dominant in the decrease in permeability below a normal stress of 5 MPa. Above this threshold stress, the effect of slaking and swelling diminishes (Fig. 10b). Thus, due to the time-dependent changes of effective self-sealing processes after initiating the tests, the permeability versus normal stress curves initially show a very rapid decrease, but then they decrease linearly with time.

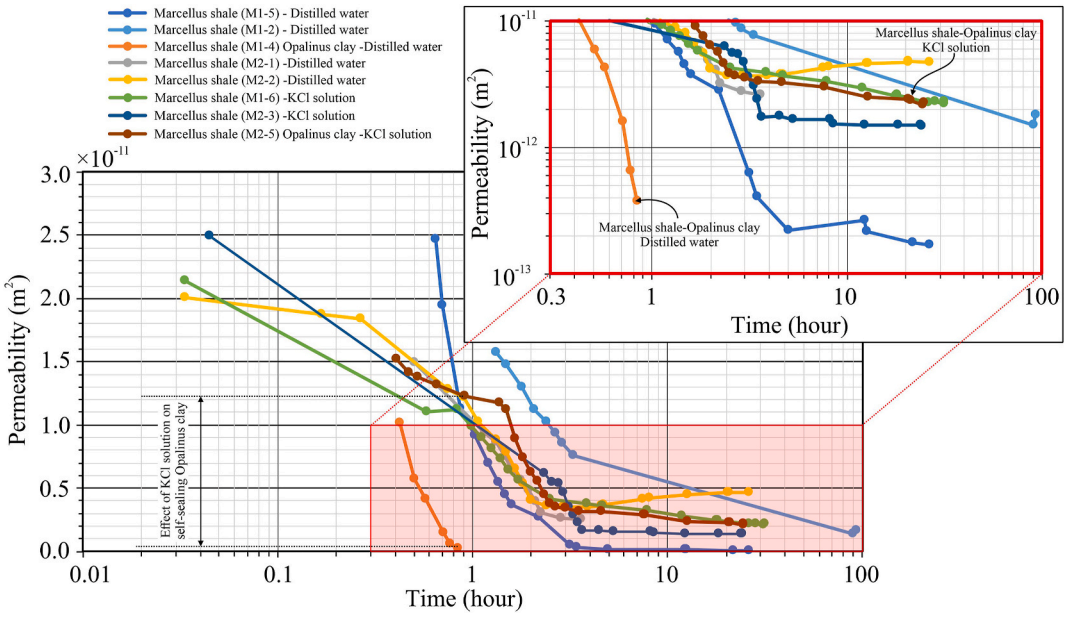

Fig. 14. Time-dependent variation in the permeability of Marcellus shale during loading.

Table 3
Data fits and empirical relations linking permeability and time for the first cycle of permeability tests.

Split samples	Stress condition	Fluid	Empirical equations
Steel platens	Loading	Distilled water	
Marcellus shale (M1-2)	Loading	Distilled water	$k = 2.53 \times 10^{-11}\, e^{-0.37t}$ ($R^2 = 0.99$)
Marcellus shale (M1-5)	Loading	Distilled water	$k = 7.08 \times 10^{-11}\, e^{-1.89t}$ ($R^2 = 0.97$)
Marcellus shale (M2-1)	Loading	Distilled water	$k = 0.94 \times 10^{-11}$ $e^{-0.034t}$ ($R^2 = 0.99$)
Marcellus shale (M2-2)	Loading	Distilled water	$k = 2.25 \times 10^{-11}$ $e^{-0.765t}$ ($R^2 = 0.99$)
Marcellus shale (M1-4)-Opalinus Clay	Loading	Distilled water	$k = 0.34 \times 10^{-11}\, e^{-7.98t}$ ($R^2 = 0.99$)
Marcellus shale (M2-5)-Opalinus Clay	Loading	KCl solution	$k = 4.93 \times 10^{-11}$ $e^{-1.021t}$ ($R^2 = 1.00$)
Marcellus shale (M1-6)	Loading	KCl solution	$k = 2.15 \times 10^{-11}$ $e^{-0.773t}$ ($R^2 = 1.00$)
Marcellus shale (M2-3)	Loading	KCl solution	$k = 2.97 \times 10^{-11}\, e^{-0.69t}$ ($R^2 = 0.95$)
Marcellus shale (M2-2)	Constant loading	Distilled water	*Internal erosion*
Marcellus shale (M2-5)-Opalinus clay	Constant loading	KCl solution	$k = 3.68 \times 10^{-12}$ $e^{-0.022t}$ ($R^2 = 0.93$)
Marcellus shale (M1-6)	Constant loading	KCl solution	$k = 4.02 \times 10^{-12}$ $e^{-0.021t}$ ($R^2 = 0.93$)
Marcellus shale (M2-3)	Constant loading	KCl solution	$k = 1.74 \times 10^{-12}$ $e^{-0.008t}$ ($R^2 = 0.71$)
Marcellus shale (M2-2)	Unloading	Distilled water	$k = 1.11 \times 10^{-14}\, e^{0.228t}$ ($R^2 = 0.91$)
Marcellus shale (M1-6)	Unloading	KCl solution	$k = 1.16 \times 10^{-18}\, e^{0.459t}$ ($R^2 = 0.99$)
Marcellus shale (M2-3)	Unloading	KCl solution	$k = 3.72 \times 10^{-15}\, e^{0.246t}$ ($R^2 = 0.91$)
Marcellus shale (M2-5)-Opalinus clay	Unloading	KCl solution	$k = 8.66 \times 10^{-15}\, e^{0.225t}$ ($R^2 = 0.99$)

k: permeability (m^2), t: time (hour).

It is well known that KCl is typically used as an inhibitor during drilling and hydraulic fracture operations to reduce well instability, shale hydration, and clogging of fractures. Fig. 10a reveals that the lowest permeability results from sample M2-3 where KCl solution is circulated – potentially as a result of mineral precipitation.

3.3.3. *Effect of heterogeneous geological structure on self-sealing behavior Marcellus shale*

The Marcellus shale formation consists of alternating clay-poor and clay-rich layers, with sampling biased towards the clay-poor competent layers. To examine the impact of these native but unsampled clay layers we substitute Opalinus clay as an agent to produce slaked particles in the flow field (Fig. 11). The split and propped Marcellus shale core is combined with an upstream fractured samples of Opalinus clay (Fig. 11) for permeability measurement at low constant upstream pressure and circulated with distilled water and KCl brine. The presence of swelling clay minerals significantly decreases the shale permeability (Fig. 11). The permeability of the sample circulated with KCl brine was higher than that exposed to distilled water at all normal stresses.

Although the KCl solution prevents the disintegration of the swelling clays, distilled water causes a heavy disintegration (shale hydration) and clogs flow channels and reduces permeability. In addition, greater proppant embedment within the Opalinus clay and the migration of micro-slaking particles from upstream to downstream cause significant self-sealing processes. Although it is quite different from the Marcellus shale in terms of swelling and slaking properties, higher permeability values are obtained from Opalinus clay when utilizing KCl brine.

3.3.4. *Permeability measurements during unloading*

We explore the role of permanent and irrecoverable fracture damage and proppant embedment during loading on the unloading response. Correspondingly, we measure permeability evolution during unloading. Significant reduction in permeability is recorded during the loading cycle (Fig. 12) that is only partially recovered during unloading. Permeabilities obtained under all conditions during the unloading phase are low.

Meyers[61] specified that while swelling-based changes in shale fractures may be reversible, the embedment caused by destructive plastic deformation of shale organic or clay components is irreversible. Similarly, even if the applied loads are removed, a significant part of these stress-dependent decreases in the permeabilities of the packed samples

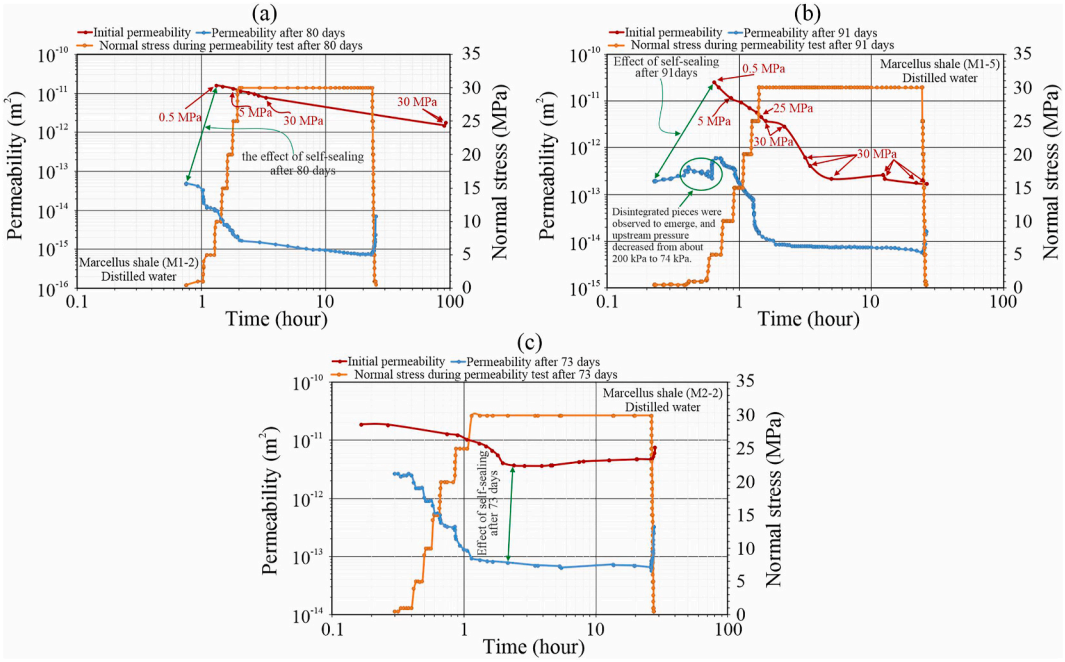

Fig. 15. Effect of self-sealing on permeability decrease for Marcellus shale retained in distilled water at temperatures ranging between 50 °C and 80 °C.

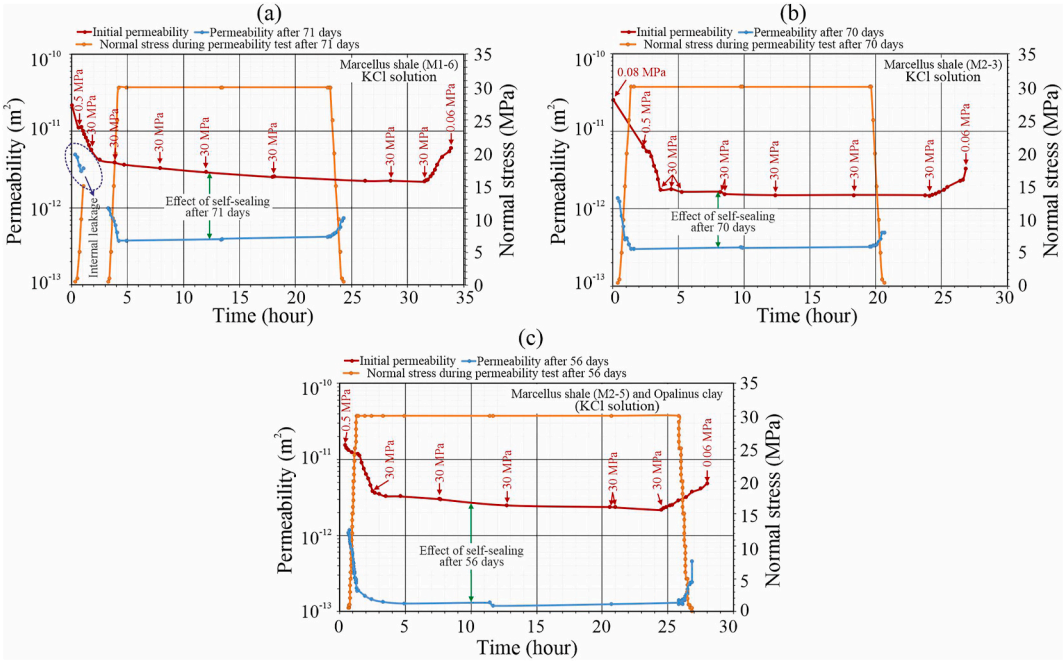

Fig. 16. Effect of self-sealing on permeability decrease in Marcellus shales retained in KCl solution at a temperature of 22 °C.

is permanent due to the elastoplastic characteristics of such clay-rich rocks. As seen in Fig. 12d and e, the effect of slaking, swelling, and embedment on the self-sealing behavior of propped fractures increases in simulated heterogeneous geological sequences where we add swelling clay minerals upstream. Permeabilities changed between 1.8×10^{-12} m^2 and 3.8×10^{-12} m^2 with a mean value of 2.7×10^{-12} after unloading (Fig. 12). Thus, it is concluded that the self-sealing percentages attributed to the compaction of the intact rock and mechanical closure of fractures range from 7.7 % to 21.6 %, with an average value of 14.5 %. All remaining reductions in permeability are anticipated to be due to slaking, proppant embedment and swelling characteristics of Marcellus shale.

3.4. Time-dependent permeability evolution – first- and second-cycle measurements

3.4.1. First-cycle measurements

We examine the long-term change in permeability of propped fractures in clay in accommodating the impacts of fracture closure, proppant embedment and slaking. We measure permeabilities in and initial cycle, with a flow hiatus of 24 h with the sample maintained under stress, then followed by a continuing second cycle of permeability measurement. Typical curves describing initial permeability measurements during the loading then unloading of normal stresses are given in Fig. 13. As a result of slaking, swelling, and proppant embedment, the permeabilities

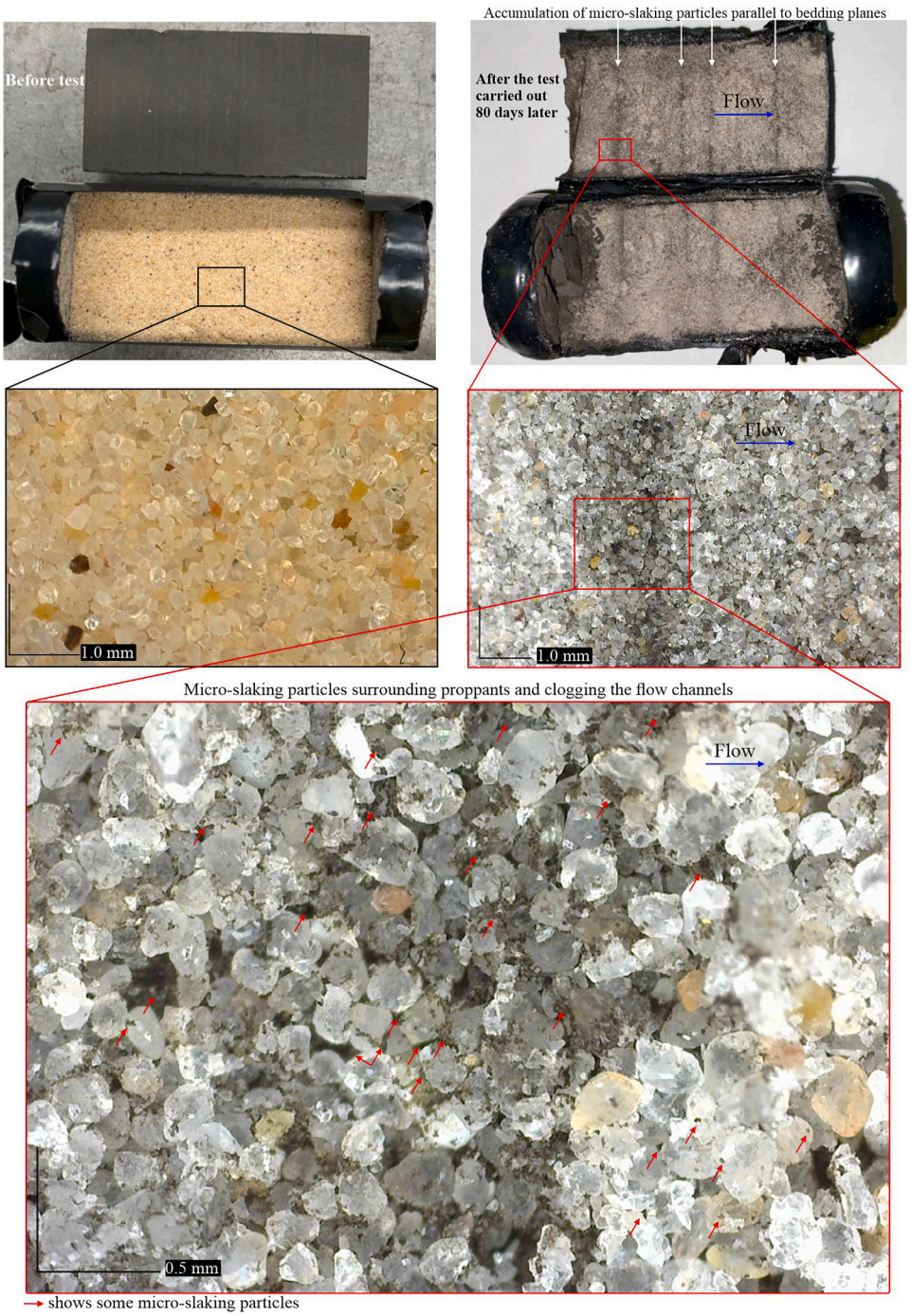

Fig. 17. Randomly scattered micro-slaking particles of Marcellus shale mixed among proppant and their arrangement in specific lines parallel to shale bedding planes (M1-2).

obtained after unloading remain significantly lower that the initial magnitudes taken at the beginning of the experiments (Fig. 13). To better observe the time dependent-change in permeability of each sample, the permeability measurements obtained during loading are given on logarithmic axes in Fig. 14.

Compared to the experiments completed with distilled water, lower permeabilities were obtained by circulating KCl solution. The propped composite samples of Marcellus shale-Opalinus clay occasionally retained higher permeabilities (Fig. 13) when circulated with KCl than those for Marcellus alone. In addition, both Figs. 13 and 14 reveal that time-dependent changes in the permeability are mainly controlled by proppant embedment and thus the effective aperture of flow channels. By using siltstone, mudstone, and conglomerate collected from the Qingxi Oilfield, Yumen (China), Wen et al.[51] noted that the time-dependent fracture conductivity can be better expressed with an empirical exponential law for a constant closure pressure (e.g., 60 MPa). They emphasized that the fracture conductivity is mainly reduced and controlled by proppant embedment; the reduction percentages of conductivity are ~65.9 % and ~87.5 % at proppant concentrations of 10 kg/m^2 and 5 kg/m^2, respectively. We use similar relations to classify our results (Table 3).

We link permeabilities in Table 3 using the relation:

$$k\left(m^2\right) = ae^{\mp bt} \tag{2}$$

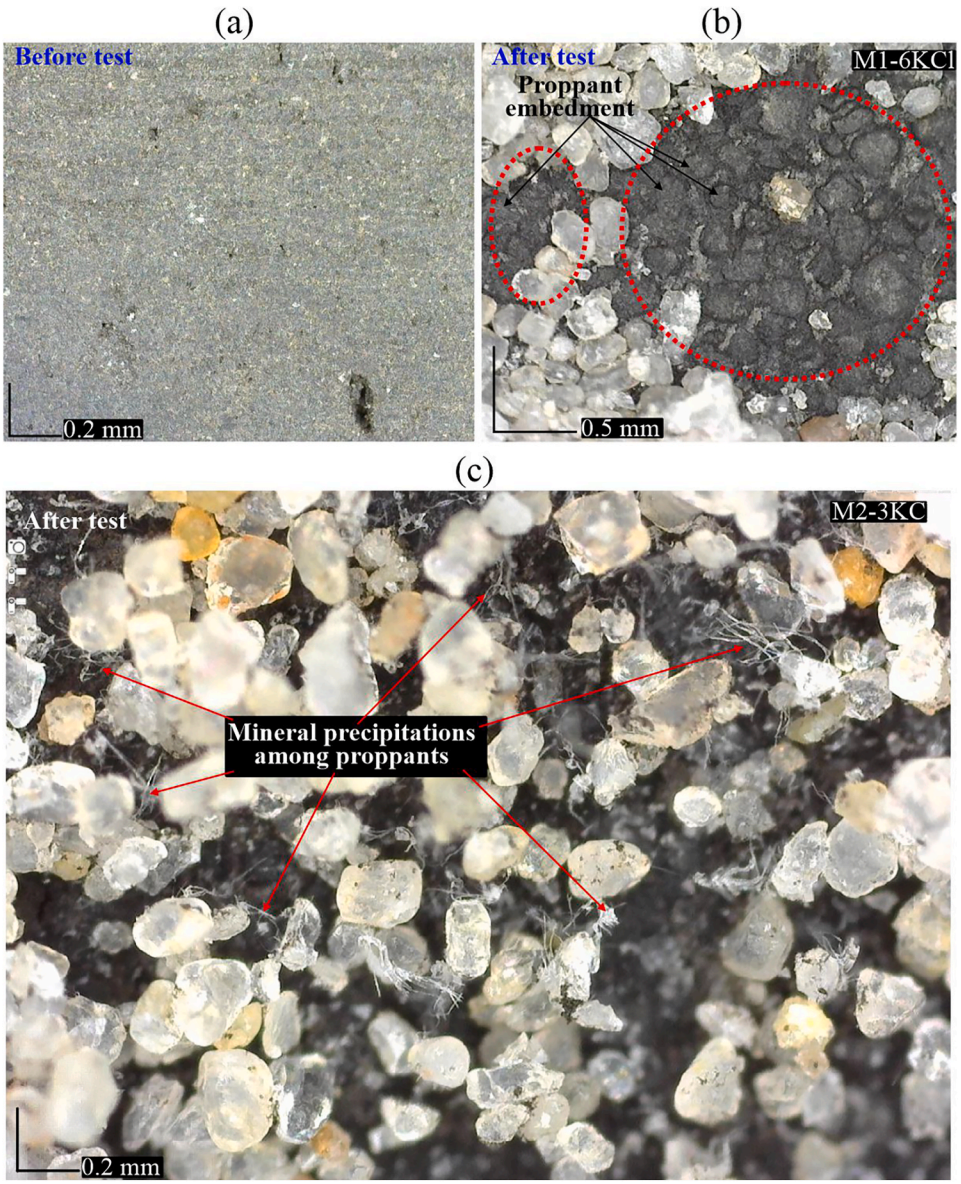

Fig. 18. a) Surface of Marcellus shale before testing, b) Permanent plastic deformations caused by proppant embedment under a normal stress of 30 MPa, c) Texture of mineral precipitation among proppants.

where t is time (hours) and a (m^2) and b (1/hours) are fitted constants. The change in these constants depends on normal stress, physical and mechanical properties of the shale, effective aperture, and proppant loading concentration. However, when the relationship between effective stress and permeability is considered, particularly those data pairs obtained during long-term permeability tests performed by Yu et al.,[4] the relative contribution of proppant loading concentration is sufficiently low to be neglected – when compared to the effects of normal stress and time. Also, time is a significant controlling factor on the self-sealing behavior of Marcellus shale in terms of including time-dependent creep deformation, slaking, and geochemical processes.

3.4.2. *Second-cycle measurements*

To examine the long-term change in permeability of propped fractures in clay to accommodate the impacts of fracture closure, proppant embedment and slaking. We measure permeabilities in an initial cycle, with a flow hiatus of 56–91 days with the sample maintained under stress, then followed by a continuing second cycle of permeability measurement. Permeability changes observed during the second-cycle are given in Figs. 15 and 16, together with the initial permeability measurements. The effects of self-sealing after 80, 91, and 73 days are given in Fig. 15a, b, and 15c, respectively, for the Marcellus shales kept in distilled water with temperatures ranging between 50 °C and 80 °C. The permeability measurements for Marcellus samples kept in KCl brine for 56–71 days at a temperature of 22 °C are given in Fig. 16. There are significant decreases in permeabilities due to self-sealing. Remarkable reductions in permeabilities by 2–4 orders of magnitude occur under different normal stresses for Marcellus shale exposed to both distilled water and KCl brine. Furthermore, no flow measurements could be taken during the second-cycle permeability measurements on split samples of Marcellus shale - Opalinus clay used to understand the effect of heterogeneity on self-sealing.

The reduction in permeability of samples circulated with distilled water, mainly controlled by proppant embedment and fracture surface deformation, lasts approximately 20–24 h at 30 MPa normal stress. Similar decreases were also obtained during initial permeability tests. However, although there is little change in permeability under a normal stress of 30 MPa in the samples placed in KCl solution (Fig. 16)

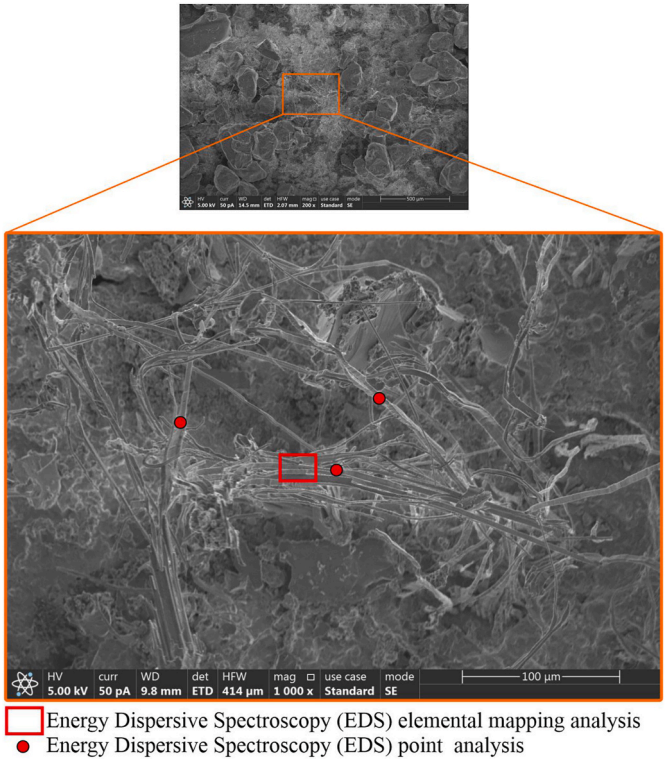

Fig. 19. The SEM image of the propped fracture and precipitated minerals.

permeability partially rebounds with time. This phenomenon may result from dissolving precipitated minerals previously left in the proppant pack. Unlike the experiment in the combined Marcellus shale - Opalinus clay sample, with distilled water, the fluid flow was obtained during permeability measurements of the same split samples kept in KCl solution (Fig. 16c). As mentioned by Shi et al.,[62] because of the effect of KCl concentration on the shale swelling and mechanical behavior, KCl solution can effectively inhibit the slaking of Marcellus shale and so prevent further disintegration and loss of strength.

3.5. Proppant embedment, micro-slaking, and mineral precipitation

We desire to visually determine changes in propped fractures and proppant packs in terms of proppant crushing, compaction, embedment, slaking and mobilization of micro-slaking particles among proppants. We examine the samples, post-test, to seek indicators of these processes using a Dino-Lite brand digital microscope. The proppant packs sandwiched within split Marcellus cores were carefully opened after second-cycle permeability tests. A typical example involving pre- and post-experiment fracture surface images of Marcellus shale after circulation with distilled water is given in Fig. 17. The break-off and deposition of micro-particles are clearly seen surrounding proppants (or present in the voids between proppants) and clog the flow channels to initiate the self-sealing of the proppant pack in the Marcellus shale. Fig. 17 shows a denser accumulation of micro-slaking particles with preferential alignments in the direction parallel to bedding planes.

Very thin shale laminae with high clay contents exist in the samples. The core samples could be readily separated along these surfaces after soaking. These disintegrated particles from thin laminae were transported into the voids within the proppants. In addition, the cohesionless proppants partially bonded by cementation after long-term exposure to water. When the undulating surface is compared with the nominal surface the of proppant pack, very high asperities were detected in parallel with heavily accumulated micro-slaked fragments along the bedding planes of laminae due to the cohesive behavior of the micro-shale particles. Similar micro-slaking particles between proppants and alignment of these disintegrated micro particles to the bedding planes were observed in split samples subjected to KCl solution.

Yakaboylu et al.[63] (2020) specified that long-duration stresses cause permanent strain in the radial direction of the parallel-bedded shales. Significant proppant embedment-based permanent plastic deformations were also observed on the fracture surface (Fig. 18b) compared with the pre-experimental surface (Fig. 18a). Furthermore, the effect of mineral precipitation, indicating self-sealing processes, was also apparent in the sample retained in the KCl solution (Fig. 18c). These precipitates are present as twisted fibers. As noted by Weaver et al.,[64] typical rates of geochemical reaction resulting in the self-sealing of fractures are quite low. Although these effects were already manifest in the short-duration experiments noted here. The onset of proppant diagenesis is apparent in Fig. 18c, which is important for further understanding the self-sealing mechanism of induced fractures.

In addition to microscopically analyzing precipitated minerals by Dino-Lite brand, Scanning Electron Microscopy (SEM) and Energy-Dispersive X-ray Spectroscopy (EDS) were also used to specify the chemical composition of precipitated twisted fibers. A typical SEM image acquired from propped surface is given in Fig. 19. To obtain a rather accurate chemical composition, one EDS elemental mapping and three EDS point analyses were carried out. The maximum, minimum, and average elemental variations of precipitated minerals are given in Table 4. The EDS analyses show that potassium chloride (KCl) brine, which represents the flowback fluids obtained in the different unconventional shale plays, precipitated along the propped fracture surface.

3.6. Comparison with other permeability evolution results for Marcellus shale

The rate and amount of self-sealing of fractures is controlled by the mineralogical and sedimentological environments of rock, pressure, temperature, fluid, and the type, size, and concentration of proppants. Tuzingila et al.[37] explored the effect of shale mineralogy, pressure, fluid saturation, bedding plane orientation, temperature, gas adsorption, and stress on its geo-mechanical properties by utilizing different experimental approaches. Based on experimental studies, Yu et al.[4] emphasized that normal stress and all parameters related to proppants (e.g., concentration, compaction, rearrangement, crushing, and embedment) play significant and systematic roles in the self-sealing evolution of induced fractures. Considering these observations and in using the same material and methods (e.g., Marcellus shale, proppant type and concentration, fluid and experimental program) to Yu et al.,[4] we compare these results. The relationships between normal stress and permeability evolution for both this study and Yu et al.[4] are given in Fig. 20a. As can be seen in this figure, the permeability-normal stress curves obtained in

Table 4
The results of EDS analyses performed on the precipitated mineral.

Statistic	Weight (%)						Atomic (%)					
	O	Al	Si	S	Cl	K	O	Al	Si	S	Cl	K
Maximum	7.98	0.32	1.85	0.40	42.80	57.66	16.89	0.41	2.29	0.44	42.74	52.06
Minimum	3.66	0.13	0.49	0.20	33.46	51.58	8.11	0.17	0.61	0.22	31.96	46.10
Average	5.43	0.24	1.16	0.28	**38.26**	**54.62**	11.76	0.31	1.43	0.31	**37.60**	**48.59**
Standard Deviation	1.85	0.08	0.59	0.09	4.00	3.24	3.75	0.11	0.73	0.10	4.50	2.75

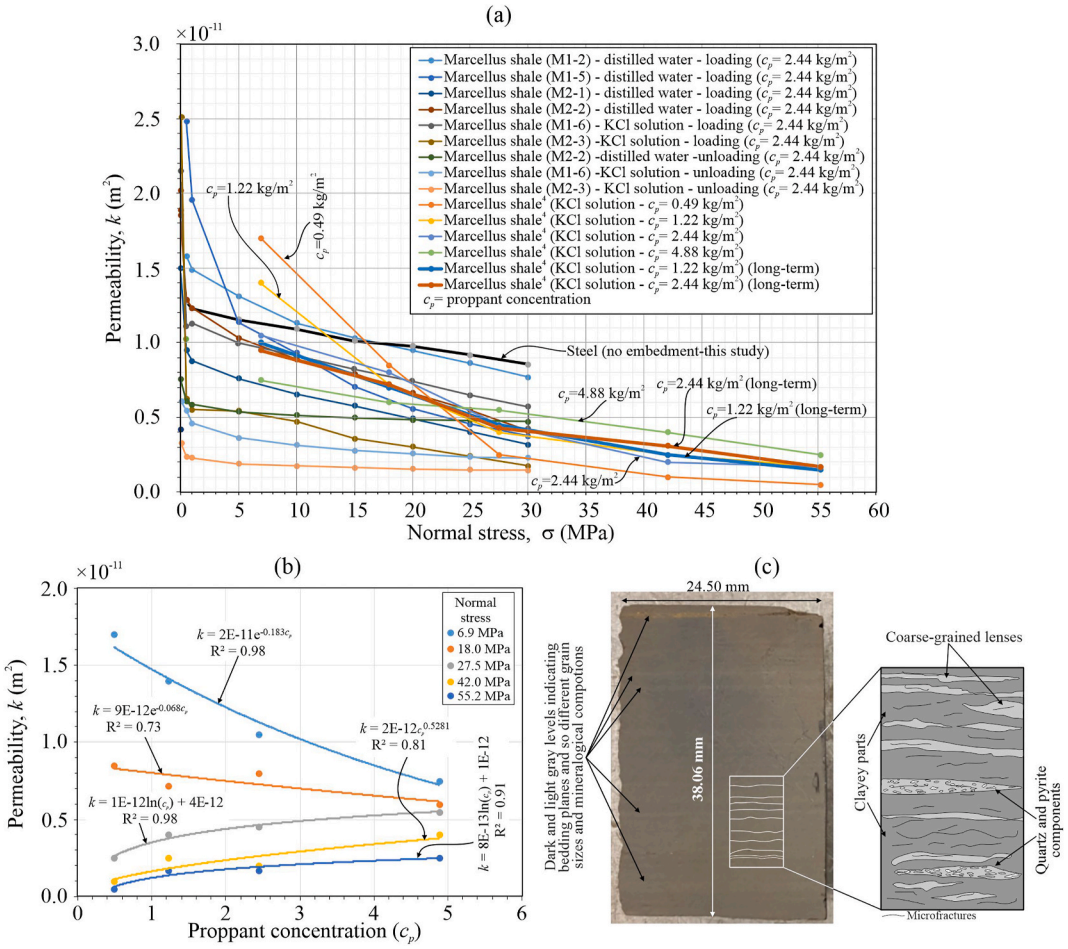

Fig. 20. a) Relationships between permeability and normal stress of Marcellus shale based on data from this study and from Yu et al.,[4] b) Effect of proppant concentrations on the permeability of propped fractures based on data obtained by Yu et al.,[4] c) Mineralogical and sedimentological heterogeneity of Marcellus shale and conceptual illustration.

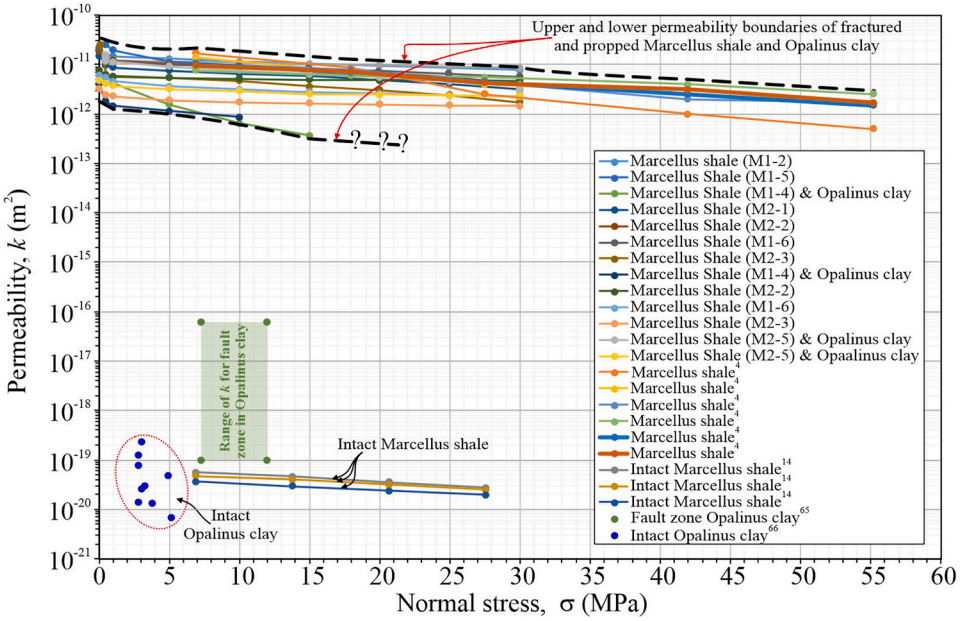

Fig 21. Effect of fracturing on the permeabilities of Marcellus shale and Opalinus clay.

both studies are compatible in terms of the slope of the curves. However, initial permeability values under low normal stress vary considerably.

Based on experimental and numerical studies, Zhang et al.[53] observed that fracture conductivities measured after fracture closure for proppant concentrations of 1.0, 1.5, and 2.0 kg/m^2 depend on the changes in the proppant concentration. However, despite utilizing a proppant concentration of 2.44 kg/m^2 in this study, the obtained permeability-normal stress curves show a wide distribution. In addition, when the permeability obtained by Yu et al.[4] under different normal stress is compared with the proppant concentrations, the data pairs on the scatterplot in Fig. 20b show no correlation. Nevertheless, when the values obtained under the same normal stress are compared with each other, there is a decrease in permeability depending on the increase in the proppant concentration up to a normal stress of 18.0–27.5 MPa, and vice versa for the relationships beyond this normal stress range. Thus, when compared with other key parameters such as mineralogical composition, stress, temperature and type of fluid, it may be concluded that the variation of permeability values, and thus the rate of self-sealing, are not as dependent on proppant concentration as previously suggested. Thus, the results reveal that the effect of proppant loading concentration on permeability evolution is minimal. It is thought that the contradiction with the results obtained by Zhang et al.[53] is due to the heterogeneity of the Marcellus Shale, which causes differential proppant embedments. When the thickness of the proppant pack is considered, the relatively excessive proppant embedments might diminish the effect of proppant loading concentration on permeability.

The results with different initial permeability values given above show that although an attempt is made to spread the proppant to a prescribed concentration on the fracture surface it is very difficult to obtain a uniform and flat distribution. Even if the same thickness of proppant is achieved across the fracture surface the sample may be disturbed during loading. Furthermore, sedimentary rocks show heterogeneity in terms of physical, mineralogical, and mechanical properties at the micro-scale due to bedding structure, sedimentation, and diagenesis processes (see Figs. 17 and 20c). According to XRD analyses performed by Yakaboylu et al.,[63] the mineralogical compositions of Marcellus shale include calcite, quartz, pyrite and dolomite phases with mineralogical heterogeneity. While less proppant embedment is expected in the coarse-grained components, micro-slaking, rapid loss of strength and elevated proppant embedment occurs in the clay-rich components. Differentials in proppant embedment along the fracture surface cause “effective aperture” values to vary due to the different proppant embedments on each fracture surface.

Hydraulic fracturing causes significant changes in the permeability of rocks. To observe the effect of fracturing on the permeability of clay-rich rocks, the permeability measurements[4,14,65,66] previously obtained from intact Marcellus shale, Opalinus clay, and a fault zone in Opalinus clay are shown in Fig. 21, together with results achieved in situ. The permeability of propped fractures may remain several orders of magnitude higher than that of intact rocks.

4. Conclusions

The following conclusions are drawn from this study:

Marcellus shale is anisotropic and heterogeneous in terms of physical, mineralogical and mechanical properties. The lithological heterogeneity results in different degrees of proppant embedment and slaking behavior, observable in the laboratory. Diagenetic bonds between layers with high clay content are broken rapidly during the first wetting-drying cycle. This typical break in diagenetic bonds is important for understanding the effect of self-sealing processes on the permeability of hydraulic fractures formed parallel to the bedding plane.

Slaking, swelling, and stress-induced processes are very effective in promoting self-sealing behavior of the Marcellus shale for normal stress in the range 2–5 MPa. Permeability sharply decreases up to the first 5 MPa in normal stress with a statistically significant linear relationship between normal stress and permeability.

The Marcellus shale shows significant slaking, swelling, and proppant embedment-based self-sealing behavior during initial permeability tests. Tests absent embedment (steel split core) show a reduction in permeability up to 63 %. In addition, the effect of slaking, swelling, and compaction on the decrease of permeability is considerably decreased for normal stresses >5 MPa, where proppant embedment and geochemical processes mainly control the self-sealing behavior. The lowest permeabilities during the initial permeability tests were achieved from packed samples circulated with KCl solution and resulting from mineral precipitation within the proppant pack.

All the permeabilities measured during the unloading phase are lower than those at equivalent stresses in the loading condition, due to significant irreversible plastic deformation and embedment of the Marcellus shale. The self-sealing attributed to the intact rock compaction and mechanical closure of fractures ranges from 7.7 % to 21.6 %, with an average value of 14.5 %. All remaining reductions in permeability are attributed to slaking, proppant embedment and swelling characteristics of the Marcellus shale. However, it should be noted that the proppant embedment, and thus the effective aperture of the fracture flow channels, are the main controlling factor of the time-dependent changes in the permeability measurements. There are statistically significant and strong exponential relationships between permeability and time.

The differences between initial and second cycle measured permeabilities reveal that time is a significant controlling factor in the self-sealing behavior, reflecting creep deformation, slaking, and long-lasting geochemical processes.

In addition to proppant-embedment-based permanent plastic deformation, microscopic examination of the propped fractures reveals dispersed micro-slaked particles, clogging flow channels within the proppant pack and initiating self-sealing in proppant pore throats. In addition to this intergranular distribution, denser accumulations of micro-slaked particles appear as stripes parallel to bedding planes in the adjacent fracture wall. Such micro-slaked structures indicate very thin shale laminae with high clay contents, confirming the important control of the lithological heterogeneity of the Marcellus shale on its self-sealing behavior.

Self-sealing processes, particularly mineral precipitation in the proppants within the Marcellus shale circulated with KCl solution over extended periods cause cementation in the originally cohesionless proppants.

Permeability versus normal stress relations from this and previous studies are comparable; however, initial permeabilities under low normal stress vary considerably. The effect of proppant loading concentrations could not be found on such variation by utilizing previously published experimental data. The lithological heterogeneity of the Marcellus shale creates proppant embedment differentiations along fracture surfaces. In addition, difficulties in achieving flat surfaces throughout the fracture surface during the proppant spreading, packed core preparation and placement in the test cell cause further limitations thus resulting in variable initial permeability values at the same proppant loading concentration.

CRediT authorship contribution statement

Zeynal Abiddin Erguler: Writing – original draft, Visualization, Validation, Methodology, Investigation, Conceptualization. **Derek Elsworth:** Writing – review & editing.

Declaration of competing interest

The authors declare that they have no known competing financial interests or personal relationships that could have appeared to influence the work reported in this paper.

Acknowledgments

This study was funded by the Scientific and Technological Research Council of Turkey (TUBITAK) 2219 with Grant No 1059B192302187.

Data availability

The data that has been used is confidential.

References

1. Nussbaum C, Bossart P, Amann F, Aubourg C. Analysis of tectonic structures and excavation induced fractures in the Opalinus Clay, mont terri underground rock laboratory (Switzerland). *Swiss J Geosci*. 2011;104(2):187–210.
2. Cikes M. Long-term hydraulic fracture conductivities under extreme conditions. In: *European Petroleum Conference*. Society of Petroleum Engineers; 1996.
3. Palisch TT, Duenckel RJ, Bazan LW, Heidt JH. Turk GA.Determining realistic fracture conductivity and understanding its impact on well performance-theory and field examples. In: *SPE Hydraulic Fracturing Technology Conference*. 2007. OnePetro.
4. Yu J, Wang J, Wang S, et al. Conductivity evolution in propped fractures during reservoir drawdown. *Rock Mech Rock Eng*. 2022:1–15.
5. Montgomery CT, Smith MB, An Z. Utilizing discrete fracture modeling and microproppant to predict and Sustain production improvements. In: *Nano Darcy Rock*. Society of Petroleum Engineers; 2020. SPE-199741-MS.
6. Sone H, Zoback M. Mechanical properties of shale-gas reservoir rocks – part 2: ductile creep, brittle strength and their relation to the elastic modulus. *Geophysics*. 2013;78(5):393–D402.
7. Barree RD, Cox SA, Barree VL, Conway MW. Realistic assessment of proppant pack conductivity for material selection. *Paper presented at the SPE Annual Technical Conference and Exhibition, Denver, Colorado*. 2003. https://doi.org/10.2118/84306-MS.
8. Briggs K, Hill AD, Zhu D, Olson K. The relationship between rock properties and fracture conductivity in the Fayetteville shale. In: *SPE Annual Technical Conference and Exhibition*. Amsterdam, The Netherlands: Society of Petroleum Engineers; 2014.
9. Alramahi B, Sundberg MI. Proppant embedment and conductivity of hydraulic fractures in shales. In: *46th US Rock Mechanics/Geomechanics Symposium*. American Rock Mechanics Association; 2012.
10. Zhang J, Zhu D, Hill AD. Water-induced fracture conductivity damage in shale formations. In: *SPE Hydraulic Fracturing Technology Conference*. 2015. OnePetro.
11. Bock H, Dehandschutter B, Martin CD, et al. Self-sealing of fractures in argillaceous formations in the context of geological disposal of radioactive waste. *NEA No*. 2010, 6184.
12. Jolley SJ, Dijk H, Lamens JH, et al. Faulting and fault sealing in production simulation models: brent Province, northern North Sea. *Pet Geosci*. 2007;13: 321–340.
13. Josh M, Esteban L, Delle Piane C, Sarout J, Dewhurst DN, Clennell MB. Laboratory characterisation of shale properties. *J Petrol Sci Eng*. 2012;88–89:107–124.
14. Heller R, Vermylen J, Zoback M. Experimental investigation of matrix permeability of gas shales. *AAPG (Am Assoc Pet Geol) Bull*. 2014;98(5):975–995.
15. Yasuhara H, Elsworth D, Polak A. A mechanistic model for compaction of granular aggregates moderated by pressure solution. *Journal of Geophysics Research*. 2003;108 (B11):2530.
16. Weaver J, Parker M, Van Batenburg D, Nguyen P. Fracture related diagenesis may impact conductivity. *SPE J*. 2007;12(3):272–281. https://doi.org/10.2118/98236-PA.
17. Pope C, Peters B, Benton T, Palisch T. Haynesville shale-one operator's approach to well completions in this evolving play. In: *SPE Annual Technical Conference and Exhibition*. Society of Petroleum Engineers; 2009.
18. Terracina JM, Turner JM, Collins DH, Spillars SE. Proppant selection and its effect on the results of fracturing treatments performed in shale formations. In: *SPE Annual Technical Conference and Exhibition*. Society of Petroleum Engineers; 2010.
19. Lee DS, Elsworth D, Yasuhara H, Weaver JD, Rickman R. Experiment and modeling to evaluate the effects of proppant-pack diagenesis on fracture treatments. *J Petrol Sci Eng*. 2010;74(1–2):67–76.
20. Zhang J, Kamenov A, Zhu D, Hill AD. Laboratory measurement of hydraulic fracture conductivities in the Barnett shale. In: *SPE Hydraulic Fracturing Technology Conference*. 2013. OnePetro.
21. Wang J, Elsworth D. Role of proppant distribution on the evolution of hydraulic fracture conductivity. *J Petrol Sci Eng*. 2018;166:249–262.
22. El Sgher M, Aminian K, Ameri S. The impact of stress on propped fracture conductivity and gas recovery in Marcellus shale. In: *Proceedings of the SPE Hydraulic Fracturing Technology Conference and Exhibition*. Texas, USA: the Woodlands; 2018: 23–25.
23. Boosari SSH, Aybar U, Eshkalak MO. Unconventional resource's production under desorption-induced effects, Petroleum, 216; 2(2), 148-155.
24. Fisher Q, Kets F, Crook A. *Self-sealing of faults and fractures in argillaceous formations: evidence from the petroleum industry*. NAB; 2013:231, 13-06.
25. Gu MZ, Sheng M, Cheng SZ, Gong FH, Li GS. Influences of shale microstructure on mechanical properties and bedding fractures distribution. *Pet Sci*. 2024;21(3): 1944–1954.
26. Fjaer E, Nes OM. The impact of heterogeneity on the anisotropic strength of an outcrop shale. *Rock Mech Rock Eng*. 2014;47(5):1603–1611.
27. Heng S, Li XZ, Liu X, Chen Y. Experimental study on the mechanical properties of bedding planes in shale. *J Nat Gas Sci Eng*. 2020;76, 10361.
28. Mokhtari M, Tutuncu AN. Impact of laminations and natural fractures on rock failure in Brazilian experiments: a case study on green River and Niobrara formations. *J Nat Gas Sci Eng*. 2016;36:79–86.
29. Jin ZF, Li XW, Jin CR, Hambleton J, Cusatis G. Anisotropic elastic, strength, and fracture properties of Marcellus shale. *Int J Rock Mech Min Sci*. 2018;109:124–137.
30. Chen TY, Feng XT, Zhang XW, Cao WD, Fu CJ. Experimental study on mechanical and anisotropic properties of black shale. *Chin J Rock Mech Eng*. 2014;33(9): 1772–1779.
31. Cho JW, Kim H, Jeon S, Min KB. Deformation and strength anisotropy of Asan gneiss, Boryeong shale, and Yeoncheon schist. *Int J Rock Mech Min Sci*. 2012;50: 158–169.
32. Gao Q, Tao JL, Hu JY, Yu XB. Laboratory study on the mechanical behaviors of an anisotropic shale rock. *J Rock Mech Geotech Eng*. 2015;7(2):213–219.
33. Cao Q, Xu H, Jiang K, et al. Differential characteristics of lithological assemblages and gas-bearing of the Permian Longtan formation mudstone in well L3, southeastern Sichuan Basin. *Geomech Geophys Geo-energ Geo-resour*. 2024;10:115.
34. Berry T, Murphy W, Paraskevopoulou C. Self-sealing of argillaceous media in the context of geological disposal of radioactive waste– a perspective from past and ongoing studies. *Geoenergy*. 2025. https://doi.org/10.1144/geoenergy2024-021. | Vol. 3 | 2025 | geoenergy2024-021.
35. Yu J, Wang J, Li Y, et al. Permeability–friction relationships for propped fractures in shale. *Rock Mech Rock Eng*. 2023;56:9085–9098.
36. Hupp BN, Donovan JJ. Quantitative mineralogy for facies definition in the Marcellus Shale (Appalachian Basin, USA) using XRD-XRF integration. *Sediment Geol*. 2018; 371:16–31.
37. Tuzingila RM, Kong L, Kasongo RK. A review on experimental techniques and their applications in the effects of mineral content on geomechanical properties of reservoir shale rock. *Rock Mechanics Bull*. 2024;3, 100110.
38. Bruner KR, Smosna R. A Comparative Study of the Mississippian Barnett Shale, Fort Worth Basin, and Devonian Marcellus Shale, Appalachian Basin. U.S. Department of Energy. DOE/NETL-2011;1478.
39. Eshkalak MO, Mohaghegh SD, Esmaili S. *Synthetic Geomechanical Logs for Marcellus Shale*. 2013. SPE 163690.
40. Li Y, Ghassemi A. Creep behavior of Barnett, Haynesville, and Marcellus shale. *ARMA*. 2012:12–330.
41. Thury M, Bossart P. The Mont Terri rock laboratory, a new international research project in a Mesozoic shale formation, in Switzerland. *Eng Geol*. 1999;52(3-4): 347–359.
42. Bossart P, Meier PM, Moeri A, Trick T, Mayor JC. Geological and hydraulic characterisation of the excavation disturbed zone in the Opalinus Clay of the mont terri rock laboratory. *Eng Geol*. 2002;66:19–38.
43. Bossart P, Thury M. Research in the mont terri rock laboratory: quo vadis? *Phys Chem Earth*. 2007;32(1-7):19–31.
44. Thury M, Bossart P. *Mont Terri Rock Laboratory. Results of the Hydrogeological, Geochemical and Geotechnical Experiments Performed in 1996 and 1997*. Swiss National Hydrological and Geological Survey, Geological; Report 23. 1999.
45. Loucks RG, Reed RM, Ruppel SC, Jarvie DM. Morphology, genesis, and distribution of nanometer-scale pores in siliceous mudstones of the Mississippian barnett shale. *J Sediment Res*. 2009;79:848–861.
46. NOGEPA. *Netherlands Oil and Gas Exploration and Production Association: Fact Sheet Fracking Nader Toegelicht*. 2011.
47. Fisher K, Warpinski N. Hydraulic-fracture-height growth: real data. *SPE Prod Oper*. 2012;27(1):8–19. https://doi.org/10.2118/145949-PA. SPE-145949-PA.
48. Lacy LL, Rickards AR, Bilden DM. Fracture width and embedment testing in soft reservoir sandstone. *SPE Drill Complet*. 1998;13(1):25–29. https://doi.org/10.2118/36421-PA. SPE-36421-PA.
49. Guo T, Zhang S, Wang L, Sui W, Wen H. Optimization of proppant size for frac pack completion using new equipment. *J Petrol Sci Eng*. 2012;96–97:1–9. https://doi.org/10.1016/j.petrol.2012.08.007.
50. Kassis S, Sondergeld CH. Gas shale permeability: effects of roughness, proppant, fracture offset, and confining pressure. In: *Presented at the International Oil and Gas Conference and Exhibition, Beijing*. 2010:8–10. https://doi.org/10.2118/131376-MS. June. SPE-131376-MS.
51. Wen Q, Zhang S, Wang L, Liu Y, Li X. The effect of proppant embedment upon the long-term conductivity of fractures. *J Petrol Sci Eng*. 2007;55(3–4):221–227.
52. Wen Q, Jin X, Subhash NS, Li Y. Experimental investigation of propped fracture network conductivity in naturally fractured shale reservoirs. In: *Presented at the SPE Annual Technical Conference and Exhibition*. 30 September–2 October. 2013. https://doi.org/10.2118/166474-MS. New Orleans.
53. Zhang F, Zhu H, Zhou H, Guo J, Bo H. *Discrete-element-method/computational-fluid-dynamics Coupling Simulation of Proppant Embedment and Fracture Conductivity After Hydraulic Fracturing*. Society of Petroleum Engineers; 2017. SPE 185172.
54. Zhang F, Fang Y, Elsworth D, Wang C, Yang X. Evolution of friction and permeability in a propped fracture under shear. *Geofluids*. 2017, 2063747.
55. Moriwaki Y, Mitchell JK. The role of dispersion in the slaking of intact clay. In: Sherard JL, Decker RS, eds. *Dispersive Clays, Related Piping, and Erosion in Geotechnical Projects*. 623. Philadelphia: ASTM STP; 1977:287–302. American Society for Testing and Materials.
56. Erguler ZA, Shakoor A. Quantification of fragment size distribution of clay-bearing rocks after slake durability testing. *Environ Eng Geosci*. 2009;15(2):81–89.
57. Erguler ZA, Ulusay R. Water-induced variations in mechanical properties of clay-bearing rocks. *Int J Rock Mech Min Sci*. 2009;46:355–370.
58. Wood LE, Deo P. A suggested system for classifying shales materials for embankments. *Bull Assoc Eng Geol*. 1975;12(1):39–55.

59. Deo P. *Shales as Embankment Materials*. PhD Thesis. West Lafayette: Purdue University; 1972.
60. Franklin JA, Chandra A. The slake-durability test. *Int J Rock Mech Min Sci*. 1972;9:325–341.
61. Meyers RA. *The Macromolecular Structure of Coal: Coal Structure*. New York: Academic Press Inc.; 1982:250.
62. Shi X, Wang L, Guo J, Su Q, Zhuo X. Effects of inhibitor KCl on shale expansibility and mechanical properties. *Petroleum*. 2019;5:407–412.
63. Yakaboylu GA, Gupta N, Sabolsky EM, Mishra B. Mineralogical characterization and strain analysis of the Marcellus shales. *Int J Rock Mech Min Sci*. 2020;130, 104345.
64. Weaver J, Rickman R, Luo H, Loghry R. *A study of proppant-formation reactions. Paper SPE 121465 Presented at the 2009 International Symposium on Oilfield Chemistry*. The Woodlands; April. 2009. https://doi.org/10.2118/121465-MS. Tx.
65. Guglielmi Y, Nussbaum C, Cappa F, Barros LD, Rutqvist J, Birkholzer J. Field-scale fault reactivation experiments by fluid injection highlight aseismic leakage in caprock analogs: implications for CO_2 sequestration. *Int J Greenh Gas Control*. 2021;111, 103471.
66. Reda SMA, Yu C, Berthe G, Matray JM. Study of the permeability in the opalinus clay series (Mont Terri-Switzerland) using the steady state method in Hassler cell. *J Petrol Sci Eng*. 2020;184, 106457.